OPUA MARINA

STAGE 2 DEVELOPMENT

MODELLING

Prepared for Far North Holdings

MET OCEAN SOLUTIONS LTD
www.metocean.co.nz

PO Box 441, New Plymouth, New Zealand
T: 64-6-7585035 E: enquiries@metocean.co.nz

MetOcean Solutions Ltd: P0176-001

October 2013

Report status

Version	Date	Status	Approved by
RevA	04/10/2013	Draft for Internal Review	Oldman
RevB	06/10/2013	Draft for internal Review	Beamsley
RevC	04/10/2013	Draft Client Review	Oldman
RevD	15/10/2013	Draft internal Review	Oldman
RevE	15/10/2013	Draft internal Review	Beamsley
RevF	16/10/2013	Draft Client Review	Oldman

It is the responsibility of the reader to verify the currency of the version number of this report.

PO Box 441, New Plymouth, New Zealand
T: 64-6-7585035 E: enquiries@metocean.co.nz

TABLE OF CONTENTS

LIST OF FIGURES

1. INTRODUCTION

Far North Holdings Limited (FNH) has commissioned MetOcean Solutions Limited (MSL) to carry out numerical modelling of the proposed extension of the Opua Marina, Bay of Islands (Figure 1.1).

The existing Marina (Figure 1.2) is located at Waimangaroa Point on the confluence of the Kawakawa River and Waikare Inlet and consists of 250 berths along with a number of swing and pile moorings outside the marina breakwater.

The proposed Marina development involves reclamation for a new hardstand area, car park, esplanade and boardwalk with associated seawall, plus dredging of around 6.5 hectare of the area south of the existing marina to create new moorings (Figure 1.3). In total 30,000 m^3 of material will be dredged from the proposed marina extension area and used for the reclamation.

This report presents output from a calibrated hydrodynamic model of the Bay of Island and quantifies the potential changes that the proposed development may have on tidal flows and sediment transport capacity within the environs.

Results from particle tracking simulations are presented to assess the potential effects of the marina extension on catchment derived sediment transport pathways and the potential pathway of contaminants from the marina.

This report is structured as follows. Section 2 gives an overview of previous reports, available data and information from the marina development completed in 1999. Section 3 provides an overview of the modelling methodologies used. Section 4 discusses model calibration and provides estimates of model skill. Section 5 outlines the bathymetry grid used to model the pre marina, Stage 1 and Stage 2 Marina. Section 6 presents and compares hydrodynamic model simulations for the proposed marina, the existing marina and conditions as they were prior to the marina being built. Results from the particle tracking simulations are also provided in this Section. Section 7 provides a summary of the main conclusion of the study. Section 8 provides report references and the report Appendix gives examples of model predictions at key sites.

LIST OF TABLES

Figure 1.1 Bay of Islands showing location of instruments (NIWA, 2010) and existing marina at the head of the Kawakawa River.

Figure 1.2 Existing Marina layout and location of Ashbys Boatyard.

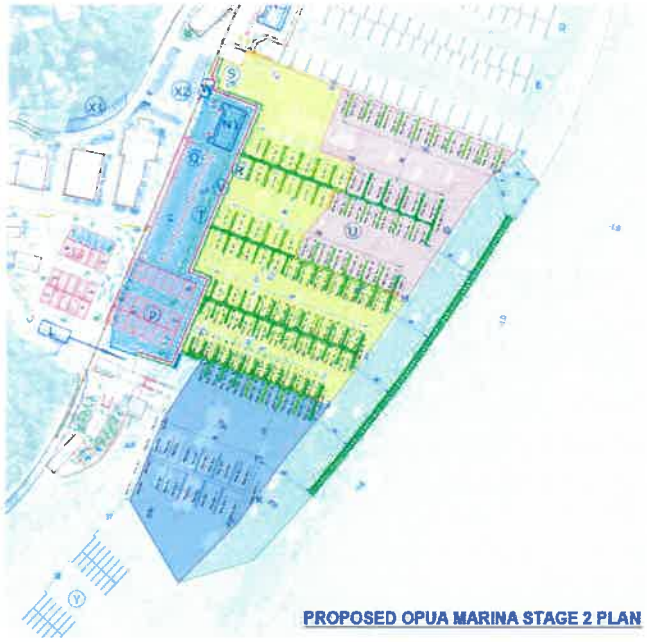

Figure 1.3 Proposed Stage 2 development of the Opua Marina showing areas of dredging and reclamation. The area to be reclaimed is shown in light blue. Area shaded in light yellow would be dredged to 2.0 m below Chart Datum. Other shaded areas would be dredged to 2.5 m below Chart Datum.

2. BACKGROUND DATA

The following section summarises data from earlier environmental assessment reports and work carried out by NIWA as part of the Bay of Islands OS20/20 project.

2.1. Kawakawa River and Waikare Inlet

Offshore of the marina the Kawakawa River has two distinct channels separated by a sandbank located mid-channel at a depth of around 1.0 m below chart datum. The spring tidal prism volume of the Kawakawa River is estimated to be 10.3×10^6 m^3. Mean and peak tidal flows offshore of the marina are estimated to be approximately 0.16 $m.s^{-1}$ and 0.30 $m.s^{-1}$ respectively (Raudkivi, 2005).

The mean annual discharge for the Kawakawa River is 10.0 $m^3.s^{-1}$ with an associated mean annual sediment yield of 339.8 $kt.y^{-1}$ (NIWA, 2010).

The catchment area of the Waikare Inlet is much less than the Kawakawa River, with a mean annual discharge for the Waikare Inlet of 0.8 $m^3.s^{-1}$ and a mean annual sediment yield of 9.1 $kt.y^{-1}$ (NIWA, 2010).

Seaward of the marina, the Kawakawa River and Waikare Inlet join to form the Veronica Channel, which is a relatively narrow deep channel which experiences peak tidal flows over 0.5 $m.s^{-1}$ (NIWA, 2010).

2.2. Water Level Variations

Tidal levels for the Opua Wharf are as follows[1]

Spring Tide range	2.1 m
Neap Tide range	1.7 m
MSL	1.4 m relative to local Chart Datum

Observed water level data from within Waikare Inlet (NIWA, 2010 – Tide Gauge Site, Figure 1.1) is given in Figure 2.1. A tidal harmonic analysis of the observed data was carried out using T-Tide (Pawlowicz et al., 2002) to provide estimates of the residual and tidal components of the water level variations (Figure 2.2). Based on the measured data, the mean spring and neap tidal ranges are 2.3 m and 1.4 m respectively, while non-tidal water levels fluctuations of around +/- 0.2 m are observed. Raudkivi (2005) provide anecdotal evidence that water levels at the marina have been observed to increase by up to 0.5 m during large river flood events.

[1] LINZ Secondary Port Tidal Data.

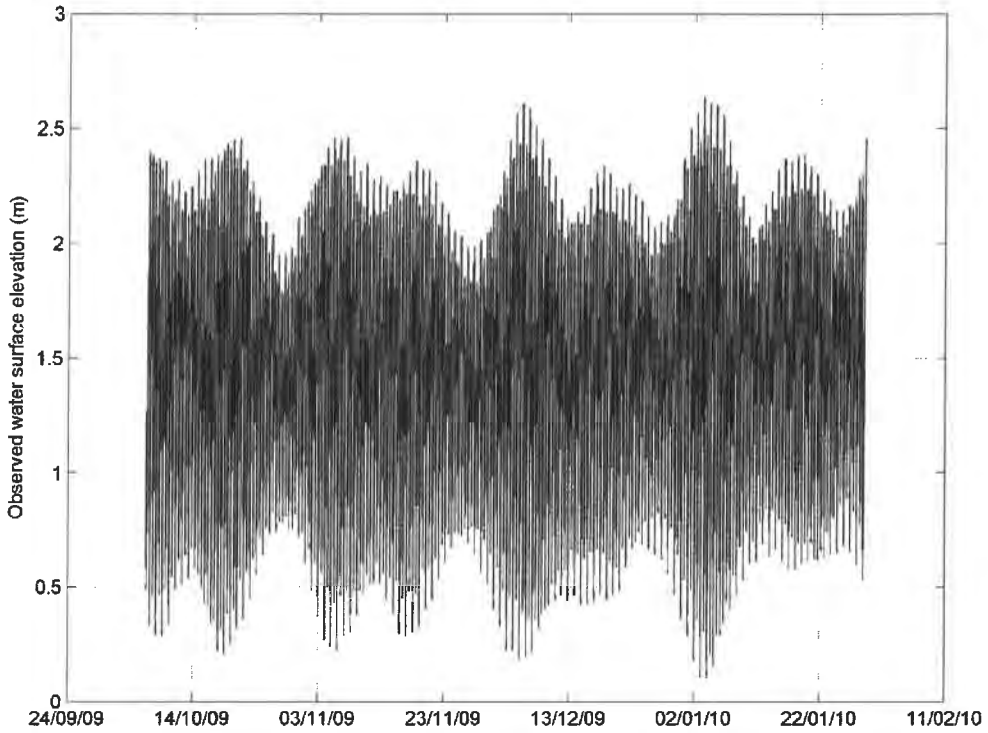

Figure 2.1 Waikare Inlet observed water surface elevations (NIWA, 2010).

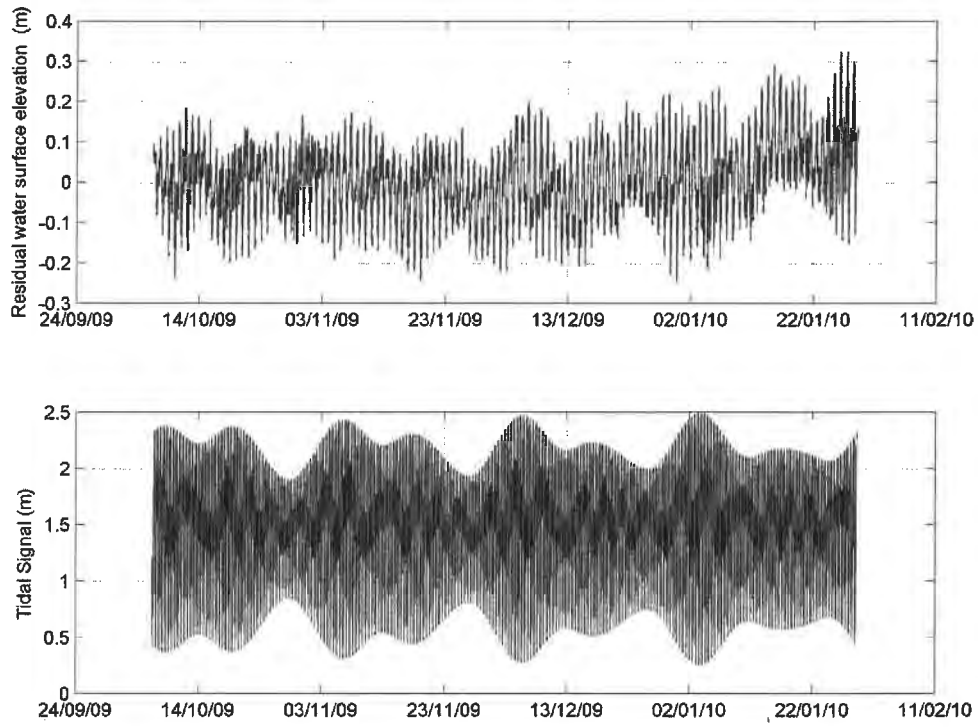

Figure 2.2 Waikare Inlet residual water surface elevations (top) and predicted tidal water level variations from observed data (NIWA, 2010).

2.3. Sediments

NIWA carried out an extensive field data programme in the Bay of Islands between October 2010 and January 2011. This period coincided with drought conditions in Northland, resulting in limited freshwater and sediment inputs. Despite this, suspended sediment concentrations of between 0.3-0.5 $kg.m^{-3}$ were observed within the Waikare Inlet (Site D1, Figure 1.1) and levels within the Veronica Channel (Site D2, Figure 1.1) were generally less than 0.1 $kg.m^{-3}$. Background levels of suspended sediment of between 0.1-0.4 $kg.m^{-3}$ were observed in the outer sector of the Bay of Islands (Site D4, Figure 1.1).

Particle size analysis from cores indicated that surficial sediments are made up of predominantly clay and silt (63 microns or less) and fine sand (< 250 micron). NIWA (2010) divided the area in the vicinity of the marina into two distinct sediment compartments. From the sediment core data, sediment accumulation rates of 2.4 $mm.yr^{-1}$ are estimated within the Waikare Inlet compartment. The range of sedimentation rates estimated from Pb_{210} isotope labelling was 1.1 to 3.5 $mm.yr^{-1}$. Mud content of the top 1 cm of cores was estimated to be 28% with the remaining 72% being made up of find sand. For the Veronica Channel sediment compartment (which includes the Kawakawa river) recent sediment accumulation rates of 3.2 $mm.yr^{-1}$ where estimated from core data. The range of sedimentation rates estimated from Pb_{210} isotope labelling was 3.5 to 14.2 $mm.yr^{-1}$. Mud content of the top 1 cm of cores was estimated to be 69% with the remaining 31% being made up of find sand.

Mean annual estimates of catchment source concentrations of 1.075 $kg.m^{-3}$ and 0.347 $kg.m^{-3}$ for the Kawakawa River and Waikare Inlet respectively were derived from catchment sediment yield and hydrological models (NIWA, 2010).

2.4. Marina Sediment Dynamics

FNC have carried out a number of surveys of the marina area since the marina was completed. For the area of the proposed extended marina (i.e. existing plus Stage 2) the estimated volumetric change between surveys carried out in 2005 and 2011 indicate an average deposition rate of +2 mm per year (DML, 2011). The change in bed level between the 2005 and 2011 surveys (in terms of an annual rate) are shown in Figure 2.3. Differences of less than 15 mm/yr have not been highlighted as the vertical accuracy of the surveys is reported to be of the order of 0.1 m (DML, 2011).

Between surveys, positive depth changes (i.e. deposition) are estimated to have occurred on the outer edge of the northern section of the marina (in the vicinity of the wave screen), the area just to the south of the Ashbys boatyard and the outer fringes of the area of the proposed marina (Figure 2.3).

Regions of negative depth change (i.e. depths have increased) and where the two surveys overlap include the inshore region of the northern part of the existing marina, the area to the south of the existing Marina and the

area around the Ashbys boatyard. No maintenance dredging has occurred in these areas over the past 10-12 years (FNC, pers. comm.).

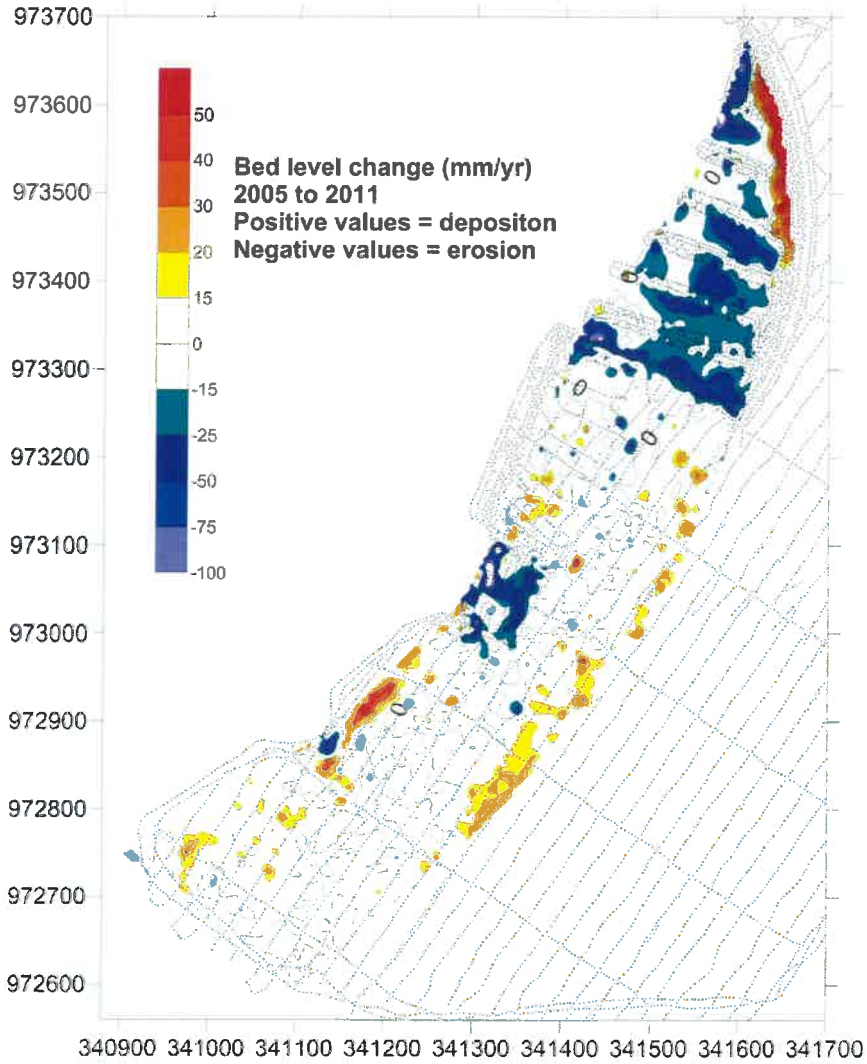

Figure 2.3 Predicted bed level change (mm/yr) based on 2011 and 2005 surveys. With 2011 survey runlines. Negative values indicate areas where bed levels have become deeper. Positive values indicate areas of deposition - where bed levels have become shallower. Changes of less than 15mm/yr (equivalent to 0.1m vertical accuracy of the surveys) are not shaded.

3. METHODS

3.1. Hydrodynamics

The hydrodynamics of Bay of Islands environs have been modelled using the hydrodynamics model SELFE. This model is a prognostic finite-element unstructured-grid model designed to simulate 3D baroclinic, 3D barotropic or 2D barotropic circulation. The barotropic mode equations employ a semi-implicit finite-element Eulerian-Lagrangian algorithm to solve the shallow-water equations, forced by relevant physical processes (atmospheric, oceanic and fluvial forcing). SELFE uses either pure terrain-

following sigma, or S-layer coordinates in the vertical, or a hybrid system using both S and Z-layers as required and uses sophisticated vertical turbulent closure models. A detailed description of the SELFE model formulation, governing equations and numerics can be found in Zhang and Baptista (2008).

3.1.1. Bathymetry grid

The model domain is shown in Figure 3.1. The finite element mesh was refined in shallow regions and in the vicinity of the Marina with mesh size ranging from 5 to 15 m. The vertical discretization used 10 sigma levels with 30, 0.7 and 10 as the hc, θb and θf constants in the Song and Haidvogel's (1994) S-coordinate system.

Three different configurations of bathymetry were used. The first uses the bathymetry data prior to Marina construction, and used data from Navy fair sheets, aerial photographs, LINZ charts and Electronic Navigation Charts. The next model configuration included the 2011 survey data (DML, 2011) and provides bathymetry as per the existing Marina. Finally the proposed reclamation and dredging for the Stage 2 development was incorporated into the bathymetry grid.

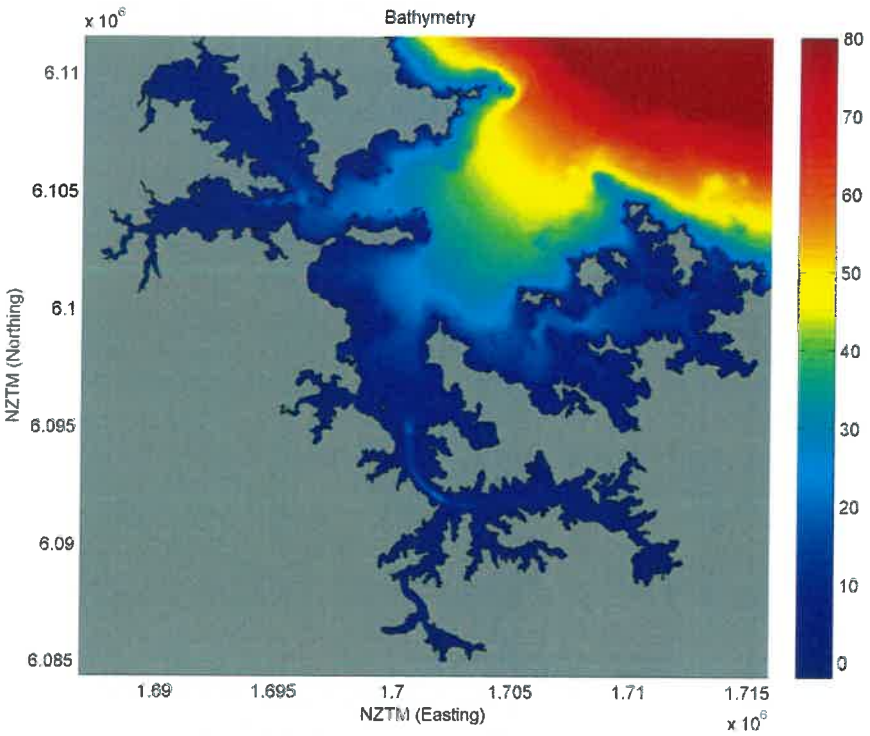

Figure 3.1 Broad scale bathymetry of the Bay of Islands.

3.1.2. Subgrid parameterisations

Vertical mixing was modelled using a k-kl model with a Kantha and Clayson (1994) stability function. A minimum and maximum diffusivity of $1x10^{-5}$ and $1x10^{1}$ m^2s^{-1} respectively was applied. A constant surface mixing length of 0.7 m was used throughout. Frictional stress at the seabed was approximated with a quadratic drag law, with the drag coefficient (CD)

determined using a bottom roughness of 0.001 m and an upper limit of CD set to 0.01.

3.1.3. Boundary and initial conditions

Tidally derived current velocities and water elevations along the open hemispheric boundary of the SELFE grid were prescribed from a NZ scale MSL-POM tidal solution. Large gradients in phase and amplitude lead to a complex tidal regime in this area, which is not fully resolved by a regular domain.

The depth variation of velocity at the boundary was approximated with a logarithmic profile using a roughness length consistent with the model bottom friction parameter. The model velocity fields were 'cold' started from rest with a ramping period of 4 days, during which the forcing and boundary conditions are gradually applied.

Mean annual flow rates for both the Kawakawa River and Waikare River were included at the sources of these two rivers.

3.1.4. Bed shear stress

Bed shear stress gives a measure of the index of fluid force due to currents near the bed. This gives a quantitative measure of the potential for sediment mobilisation and subsequent transport. Estimates of bed shear stress (τ) can be defined using the quadratic stress law (Christoffersen and Jonsson, 1985) which relates the average bed shear stress to depth-averaged flow;

$$\tau = C_D \, \rho_w \, \sqrt{(u^2 + v^2)} \qquad (1)$$

Where ρ_w is the density of water, u is the east-west component of the depth-average velocity, v is the north-south component of the depth-averaged velocity and C_D is the drag coefficient as defined by Gross et al. 1999;

$$C_D = \left(\frac{0.4}{\log(\frac{z}{z_0})} \right)^2 \qquad (2)$$

Where z is the total water depth and z_o is the roughness length.

3.1.5. Sediment transport capacity

Sediment transport capacity is defined using Soulsby and van Rijn formula (Soulsby, 1997) which combines bed load and suspended sediment load in the east-west (Q_x) and north-south (Q_y) component as follows;

$$Q_y = A_s u \, (\sqrt{u^2} - \mathrm{U}_{cr})^{2.4} \qquad (3)$$

$$Q_x = A_s v (\sqrt{v^2} - \mathrm{U}_{cr})^{2.4} \qquad (4)$$

Where U_{cr} is the critical bed shear stress velocity obtained following Van Rijn (Soulsby, 1997 p.176):

$$U_{cr} = 0.19 d_{50}^{0.1} \log 10(4h/d_{90}) \quad \text{if } d_{50} \leq 0.5 \text{ mm} \qquad (5)$$

$$U_{cr} = 8.5 d_{50}^{0.6} \log 10(4h/d_{90}) \quad \text{if } d_{50} > 0.5 \text{ mm} \qquad (6)$$

Where d_{50} is the median grain size of the sediments being considered, d_{90} is the 90th percentile grain size of the sediments being considered and h is the water depth. Based on the NIWA data a d_{50} of 60 micron and a d_{90} of 100 micron were assumed.

A_s is the combined bed load (A_{ss}) and suspended sediment load (A_{sb}) defined as;

$$A_{sb} = 0.05.h\left(\frac{d_{50}/h}{\Delta.g.d_{50}}\right)^{1.2} \qquad (7)$$

A_{ss} is the suspended load multiplication factor;

$$A_{ss} = 0.012.d_{50}.\frac{D_*^{-0.6}}{(\Delta.g.d_{50})^{1.2}} \qquad (8)$$

with the dimensionless particle size (D_*) defined as;

$$D_* = \left(\frac{g.\Delta}{\nu^2}\right)^{1/3}.d_{50} \qquad (9)$$

where $\Delta = \frac{\rho_s - \rho_w}{\rho_w}$, ρ_s is the density of sediment, g is gravitational constant, and ν is the kinematic viscosity (taken as 1e-6 m^2/s).

3.2. Particle tracking

The transport and dispersion of conservative tracers from the Stage 2 marina area or catchment source has been simulated using a lagrangian based particle tracking model (PartTracker) which couples to the flow-fields from the calibrated hydrodynamic ocean model.

This model has been jointly developed by MetOcean Solutions Ltd and the Cawthron Institute (Knight et al. 2009). PartTracker calculates the Lagrangian paths of particles over a given time step by numerical integration within the time-varying velocity field provided by the hydrodynamic ocean model. Velocity estimates are linearly interpolated in time and space from discrete time "snapshots" of predicted flow fields. The numerical scheme then calculates an error estimate using the difference between the 5th order and embedded 4th order Runge-Kutta solutions (Press et al.1992). If the calculated error estimate for a given particle is greater than a predefined value (1 mm is used in this study) then the model time step is reduced until the required accuracy is achieved.

If a particle passes the error check, it is also tested to ensure that the distance moved is not greater than a predefined value (50 m is used in this

study). This ensures that particle movements do not jump over velocity data in areas of high flow. As with the error check, if this distance is exceeded, then the model time step is lowered accordingly. This ensures that the particles accurately reproduce streamlines within the current fields.

After calculation of the Lagrangian displacement is completed for all particles, an additional random displacement is added to simulate diffusion processes. The random component is determined from a classical diffusion equation (García-Martínez & Flores-Tovar, 1999; Lonin, 1999) as:

$$\begin{aligned} T_x &= R\sqrt{(6D_x\Delta t)} \\ T_y &= R\sqrt{(6D_y\Delta t)} \\ T_z &= R\sqrt{(6D_z\Delta t)} \end{aligned} \qquad (10)$$

where *Tx*, *Ty* and *Tz* are the random turbulent components in the horizontal and vertical. *R* is a uniformly distributed random number and Δt is the model timestep. *Dx* and *Dy* are the diffusivity in the horizontal directions and *Dz* is the diffusivity in the vertical direction – all calculated from the eddy diffusivity in the hydrodynamic model.

Concentration maps are produced from the particle distribution at each output time-step of the particle tracking model. A kernel method with variable bandwidth was used to reconstruct the concentration at each spatial location in a regular 50 m grid. The use of a variable bandwidth (kernel size) attempts to represent true variability of spatial concentration, while minimising statistical variability that inevitably occurs away from the source due to a necessarily finite number of particles. A small kernel is used in regions of high numbers of particles, where it is statistically appropriate to infer relatively small scale changes in concentration. A larger kernel in areas of low density prevents unrealistically high concentrations around the precise (but partially random) locations of a few isolated particles.

The concentration(C) is computed at each time-step and regular grid location as:

$$C(x,y,t) = \sum_{i=1}^{n} \frac{m_i}{\lambda_x(x,y,t)\lambda_y(x,y,t)} K\left(\left|\frac{x_i - x}{\lambda_x}\right|\right) K\left(\left|\frac{y_i - y}{\lambda_y}\right|\right) \qquad (11)$$

where n is the total number of particles, λ_x, λ_y are the kernel bandwidth in the x and y directions and K is the kernel function. The loading, m_i, for each particle depends on the quantity being simulated.

Following Vitali et al. (2006), a Epanechnikov kernel function is used:

$$K(q) = \begin{cases} 0.75(1-q^2), & |q| \le 1 \\ 0 & |q| > 1 \end{cases} \qquad (12)$$

with q as the ratio of a particle distance from node to the bandwidth length scale. A receptors based method (a modification of their *RL3*) is used to define the bandwidths. The bandwidths are defined as twice the standard

deviation of the projected distance in the x or y direction of any particles in the neighbourhood of a grid point. The neighbourhood is defined as the region enclosing the 1/20th closest particles. The aspect ratio (e.g. λ_x/λ_y) of the bandwidths are limited to be no greater than 5:1 to prevent unrealistically elongated kernels, with the smaller value increased.

3.3. Model skill score

As a guide to defining the model skill, methodologies outlined in Zhang et al. (2010) are used to provide the following quantitative statistics:

Mean absolute error: $$\overline{|x_m - x_o|} \quad (13)$$

RMS error: $$\sqrt{\overline{(x_m - x_0)^2}} \quad (14)$$

Bias: $$\overline{x_m - x_0} \quad (15)$$

Model Skill: $$1 - \frac{\overline{(x_m - x_o)^2}}{\left[\overline{(x_m - \overline{x_o})} + \overline{(x_o - \overline{x_o})}\right]^2} \quad (16)$$

Where x_o is the observed data and x_m the modelled data and a bar indicates an average over all data and/or data pairs.

4. MODEL CALIBRATION

A model simulation covering the period 11th October 2008 – 13th November 2008 was run using the setup as described in Section 3.1. This provided estimates of tidally driven currents and water level variations across the whole model domain (Figure 3.1). Using the observed tide gauge records and current meter data (Figure 1.1) estimates of the tidal component of currents and water level variations for the modelled time period were determined using tidal harmonic analysis (Pawlowicz et al., 2002).

Adjustments to bed roughness were carried out to provide a good fit between the observed and predicted tidal water level fluctuations. The final global bed roughness value used was 0.001 m. The QQ plot of the observed and predicted tidal water levels at the tide gauge site in Waikare Inlet is given in Figure 4.1. The distribution of predicted tidal water levels is in very good agreement with the observed data. The skill score estimates for the model predictions are presented in Table 4.1 and indicate the model faithfully captures the fluctuations in tidally driven water elevations.

QQ plots for current meter data at Site D4 (Figure 1.1) are shown in Figure 4.3 (*u*; east-west component and *v*; north-south component) and Figure 4.4 (Tidal speed). Tabulated skill score estimates (Table 4.2-Table 4.4) show that the model faithfully captures both the *u* and *v* component of the tidal velocity.

No current meter data was available near the marina site – therefore a quantitative calibration of currents in and around the marina was not possible. However, the good calibration achieved in terms of both water level fluctuations and tidal current at the outer sites indicate that the exchange of oceanic water into and out of the Veronica Channel is being

well modelled. In addition, the good water level calibration achieved at the Waikare Inlet site indicates the volume of water being transferred into and out of the area in the vicinity of the marina is being well modelled. Because the model uses high quality bathymetry data (Section 3.1.1) it is expected that that modelled currents in the vicinity of the Marina are well predicted by the model.

Table 4.1 Skill score estimates for tidal water levels variations, Waikare Inlet and Tapeka Point tide gauges (Figure 1.1).

	Waikare Inlet	Tapeka Point
Bias	0.010	<-0.001
Mean Absolute Error	0.066	0.108
Root Mean Square Error	0.083	0.130
SKILL	0.861	0.786
Percentage of predictions that lie within +/- 10 cm of observations	73.8	49.8
Percentage of errors that are greater than + 10 cm	16.0	25.2
Percentage of errors that are less than -10 cm	10.2	25.0

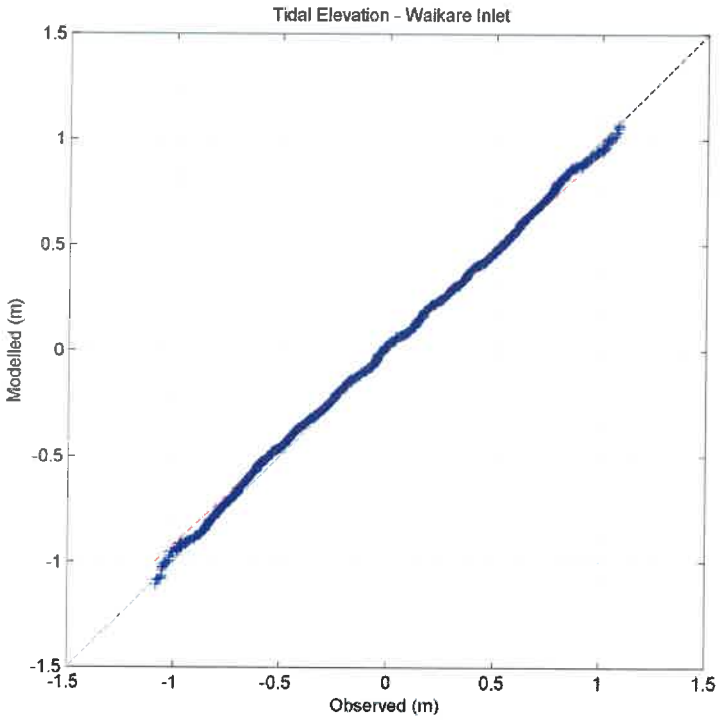

Figure 4.1 QQ plot of observed and predicted tidal water level variations at the Waikare Inlet tide gauge site (Figure 1.1).

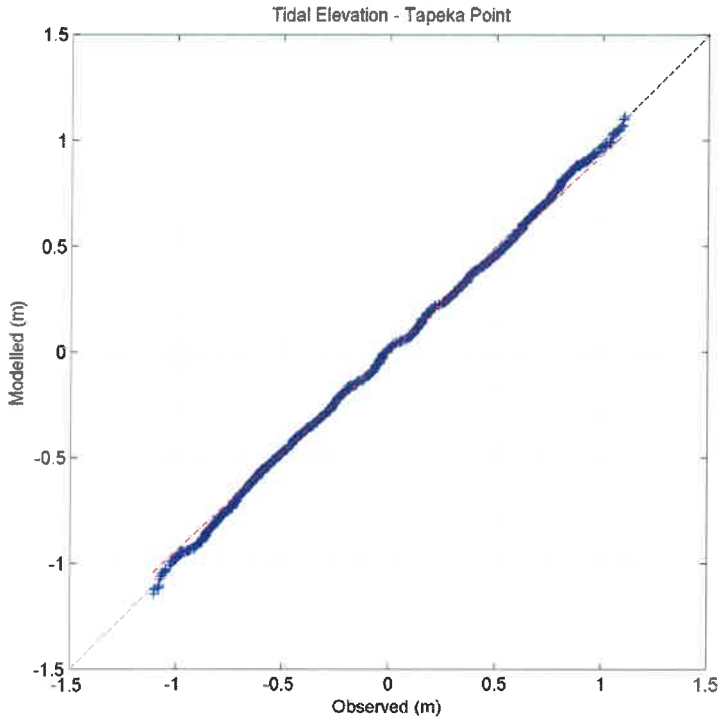

Figure 4.2 QQ plot of observed and predicted tidal water level variations at the Tapeka Point tide gauge site (Figure 1.1).

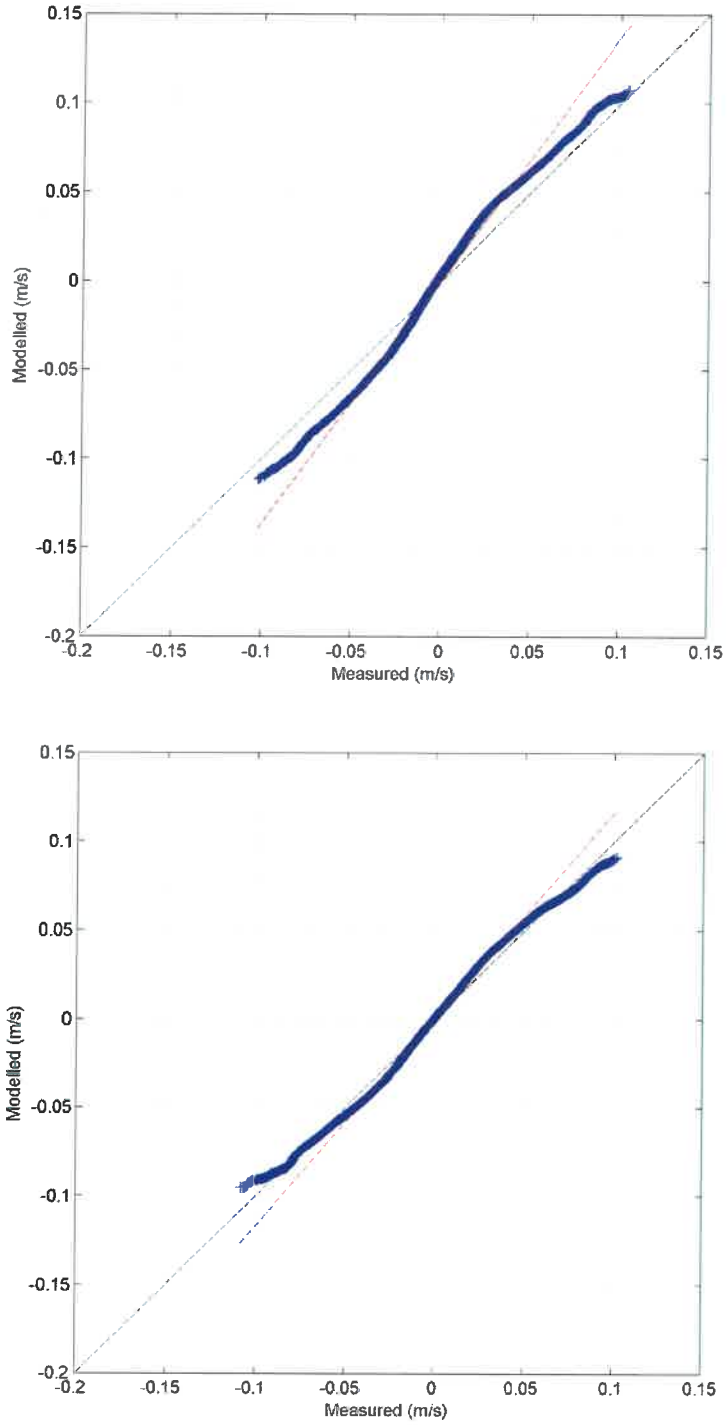

Figure 4.3 QQ plots for observed and predicted depth-averaged U (north-south) component of tidal current (top panel) and V (north-south) component of tidal current (top panel) at Site D4 (Figure 1.1). Site is in 25 m of water.

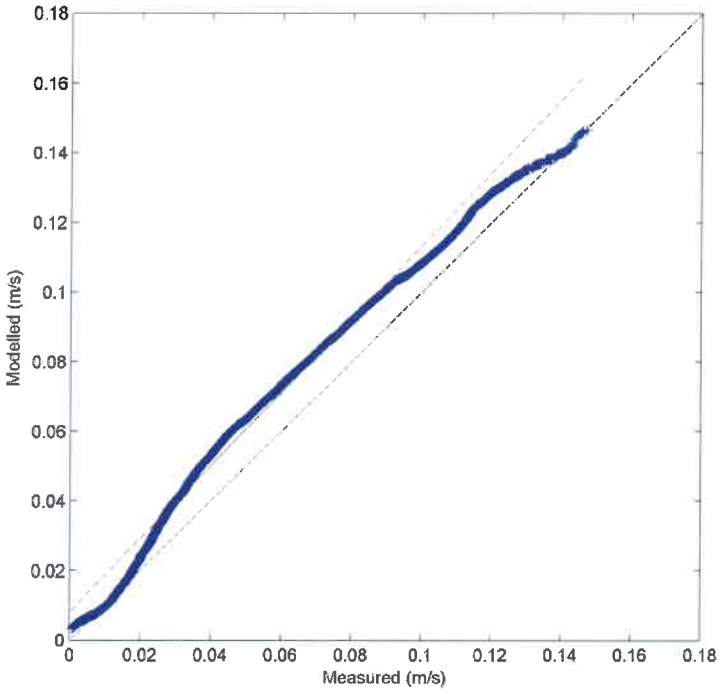

Figure 4.4 QQ plots for observed and predicted depth-averaged tidal current speed at Site D4 (Figure 1.1).

Table 4.2 Model skill score for the U component (east-west) of tidal current at Site D4 (Figure 1.1).

U tidal component	
Bias	< -0.001
Mean Absolute Error	0.022
Root Mean Square Error	0.027
SKILL	0.407
Percentage of predictions within +/- 2 cm/s of observations	52.16
Percentage of errors that are greater than + 2 cm/s	24.94
Percentage of errors that are less than - 2 cm/s	22.90

Table 4.3 Model skill scores for the V component (north-south) of tidal current at Site D4 (Figure 1.1).

V tidal component	
Bias	< -0.001
Mean Absolute Error	0.019
Root Mean Square Error	0.023
SKILL	0.492
Percentage of predictions within +/- 2 cm/s of observations	57.96
Percentage of errors that are greater than + 2 cm/s	2.11
Percentage of errors that are less than – 2 cm/s	20.10

Table 4.4 Model skill scores for tidal speed at Site D4 (Figure 1.1).

Tidal Speed	
Bias	0.010
Mean Absolute Error	0.025
Root Mean Square Error	0.031
SKILL	0.323
Percentage of predictions within +/- 2 cm/s of observations	48.42
Percentage of errors that are greater than + 2 cm/s	3.65
Percentage of errors that are less than – 2 cm/s	16.12

5. BATHYMETRIC CHANGES

Data for the broad scale bathymetry (Figure 3.1) was derived from collating data from sources as listed in

Table 5.1. In the vicinity of the Marina three bathymetry configurations were used – pre marina, Stage 1 Marina and Stage 2 development. Figure 5.1 shows the finite-element grid and bathymetry for the pre marina configuration. For the Stage 1 Marina bathymetry survey data from the 2011 DML survey (DML, 2011) was merged with the pre marina bathymetry to give the bathymetry shown in Figure 6.2. Finally the proposed reclamation and dredging associated with the Stage 2 development was incorporated into the bathymetry to give the bathymetry shown in Figure 5.3. The differences in bathymetry between the Stage 1 Marina and that of the Stage 2 development are shown in Figure 5.4.

Table 5.1 Bathymetric data sources used.

Bathymetry Data	Source
Electronic Navigation Charts	LINZ
Survey data	DML
LIDAR	Northland Regional Council
Multi Bean Echo Sounder	NIWA Ocean Survey 20/20
Single Bean Echo Sounder	LINZ
Fare sheets	LINZ
API (Aerial photographic interpretation)	In house

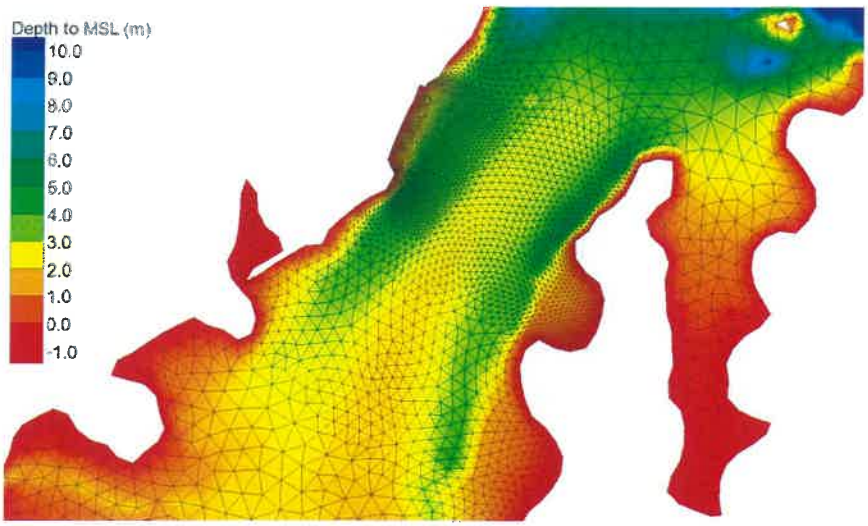

Figure 5.1 Hydrodynamic model grid showing pre marina bathymetry configuration. Depths are in terms of Mean Sea Level (1.4 m above Chart Datum).

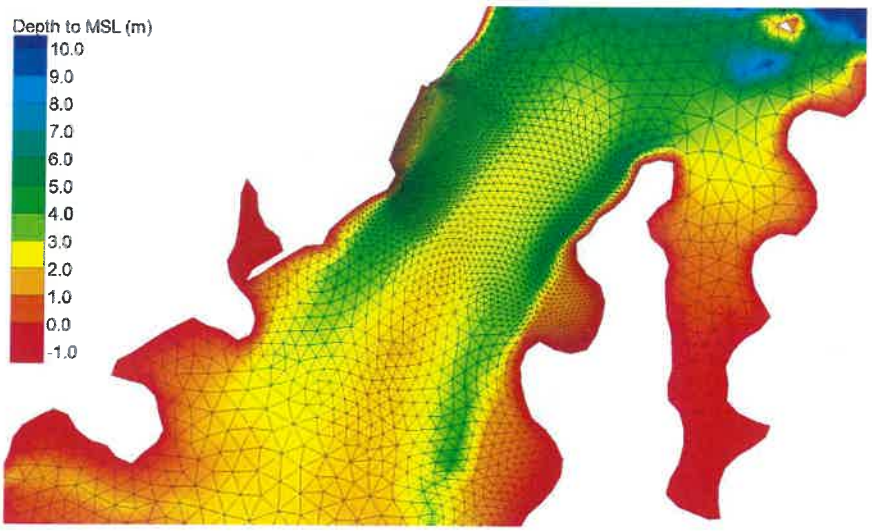

Figure 5.2 Hydrodynamic model grid showing Stage 1 marina bathymetry configuration. Depths are in terms of Mean Sea Level (1.4 m above Chart Datum).

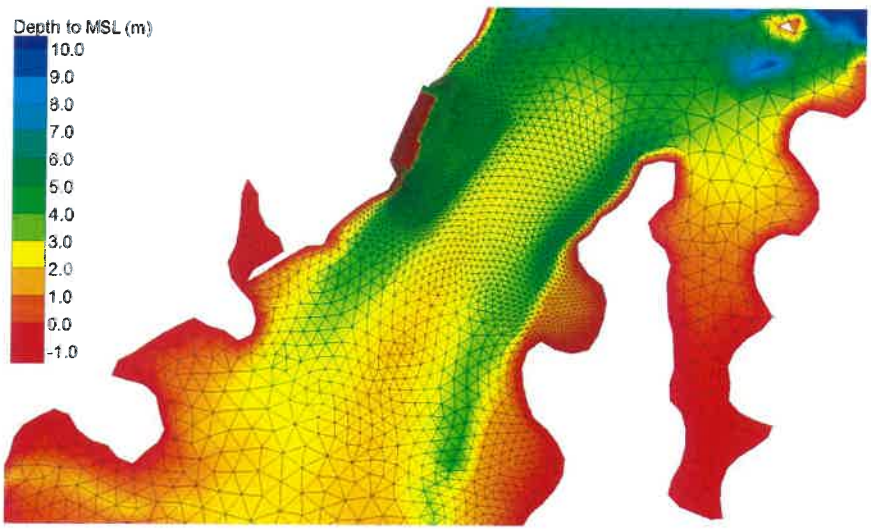

Figure 5.3 Hydrodynamic model grid showing Stage 2 marina bathymetry configuration. Depths are in terms of Mean Sea Level (1.4 m above Chart Datum).

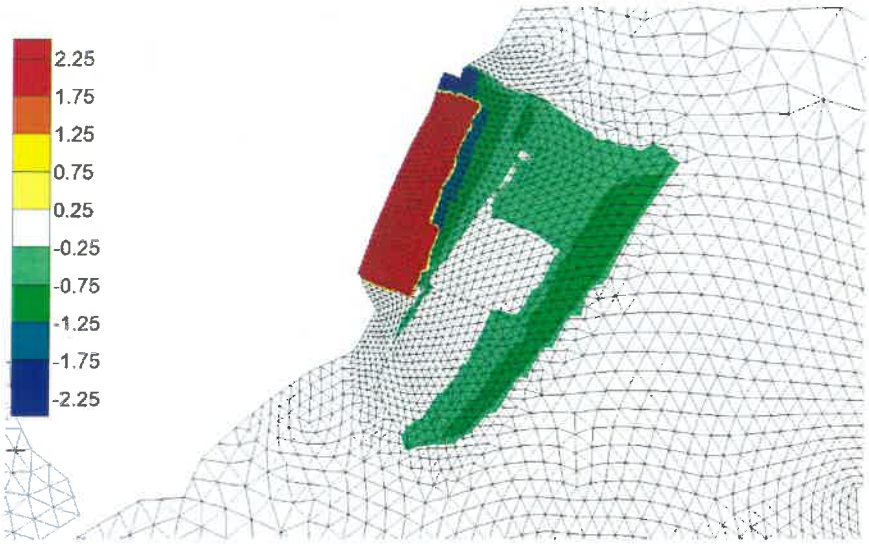

Figure 5.4 Hydrodynamic model grid showing differences in bathymetry between Stage 2 Marina development and the existing Stage 1 Marina.

6. RESULTS

6.1. Hydrodynamics - Pre Marina

The following section of the report gives an overview of the results from the hydrodynamic model run with the pre marina bathymetry configuration.

At a broad scale it can be seen that predicted peak tidal flows under neap tides are generally less than 0.3 $m.s^{-1}$ with maximum peak flows predicted to occur within the Veronica Channel and in an area just to the south of the Marina site (Figure 6.1). In the vicinity of the Marina site (Figure 6.2) peak neap tidal flows are predicted to be generally less than 0.2 $m.s^{-1}$, with slightly stronger flows on the ebb tide towards the Marina site.

Under spring tides predicted tidal flows are much stronger than under neap tides with broad scale peak tidal flows greater than 0.5 $m.s^{-1}$ in many places (Figure 6.3). In the vicinity of the Marina site (Figure 6.4) peak flows of less than 0.35 $m.s^{-1}$ occur with stronger flows on the ebbing tide within the western channel of Kawakawa River.

Predicted net currents (i.e. the net predicted current over a full tidal cycle) in the vicinity of the Marina site indicate a small south-easterly directed residual current in the channel to the east of the Marina site and a north-easterly net current just offshore of the Marina Site (Figure 6.5). To the south of the Marina site net currents within the main channel of the Kawakawa River of around 0.02-0.03 $m.s^{-1}$ are expected.

The mean bed shear stress for neap and spring tides (derived from integrating Equation 1 over a tidal cycle) are shown in Figure 6.6. This parameter gives a measure of the ability of currents to mobilise sediments. The higher mean bed shear stress values within the Veronica Channel and offshore and south of the Marina site indicate that sediment arriving within these areas is less likely to settle (especially during spring tides). Sediments arriving in areas with low mean bed shear stress are more likely to settle and not be remobilised. Actual deposition rates will depend on how fine grain sediments are transported from catchments and through the system – this is addressed in Section 6.5.

The predicted sediment transport capacity (derived from Equations 3-9) for both a neap and spring tidal cycle are presented in Figure 6.7. Here the role that both water depth and time that shear stress exceeds a critical value (i.e. Equations 3 & 4) become quite evident. Along the western side of the Kawakawa River maximum predicted sediment transport capacity occurs due to the combination of northward directed net currents (Figure 6.5) and the strength of the tidal flows that occur in relatively shallow water in this area (Figure 6.2). Further offshore the sediment transport capacity is reduced within the Kawakawa River. Other areas where sediment transport capacity is predicted to be relatively high are on the eastern side of the Kawakawa River and to the south of the Marina site (where the net sediment transport capacity is directed to the west, consistent with the predicted net currents in this area – Figure 6.5).

Time-series plots of predicted depth-averaged currents at ten sites in the vicinity of the Marina site (Fig. 5.8) are given in Appendix 1. Table 6.1

gives the location of these sites and the predicted mean speed over the full one-month simulation.

Table 6.1 Location of hydrodynamic time series sites (Fig. 5.8) and predicted mean speed for the pre marina bathymetry configuration.

Site Identifier	Latitude (WGS84)	Longitude (WGS84)	RMS speed ($m.s^{-1}$)
1	-35.3095	174.1200	0.210
2	-35.3140	174.1227	0.123
3	-35.3168	174.1209	0.136
4	-35.3207	174.1171	0.097
5	-35.3145	174.1248	0.126
6	-35.3176	174.1230	0.131
7	-35.3224	174.1183	0.155
8	-35.3161	174.1266	0.047
9	-35.3186	174.1244	0.069
10	-35.3236	174.1211	0.084

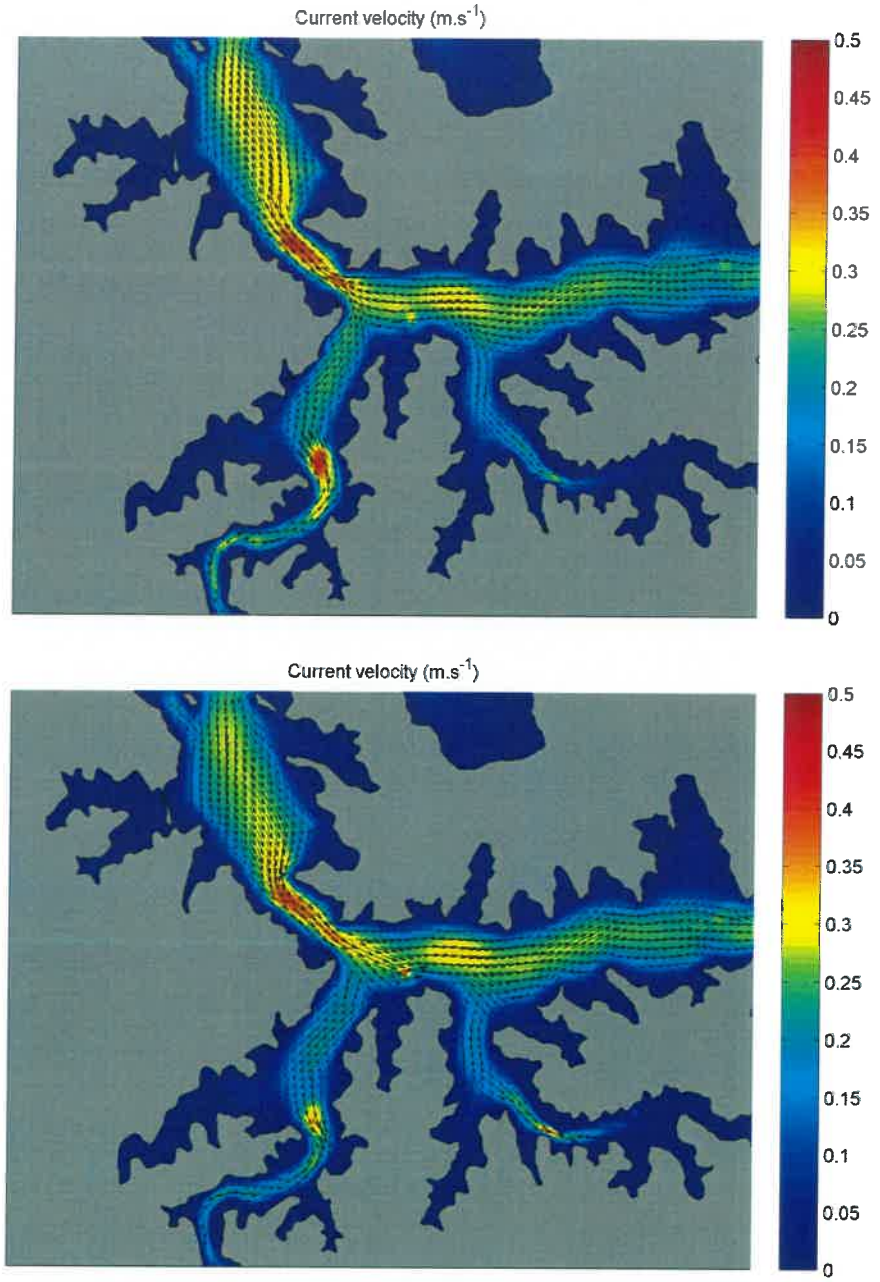

Figure 6.1 Broad scale depth-averaged peak neap ebb (top panel) and peak neap flood (bottom panel) tidal currents. Bathymetry representative of conditions prior to the development of the Opua Marina.

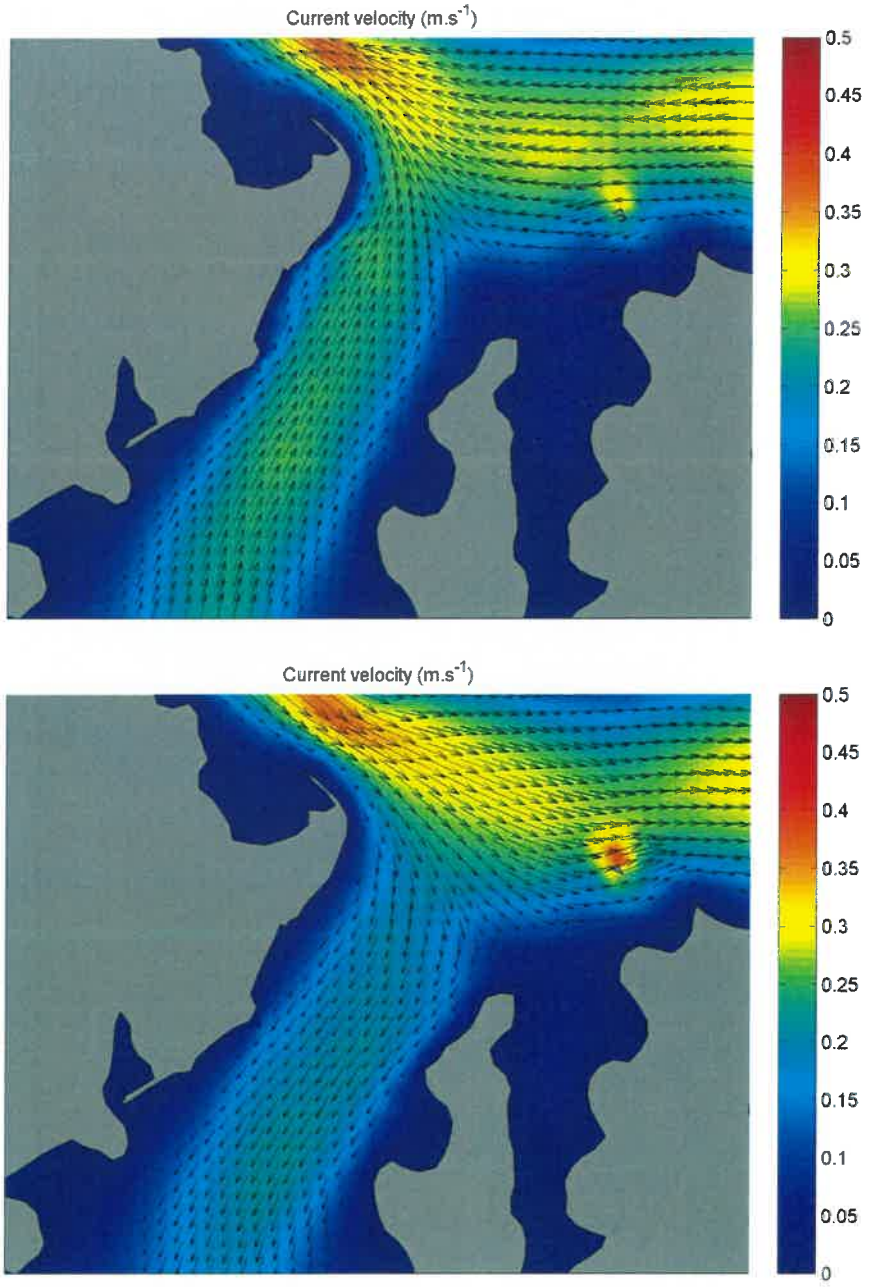

Figure 6.2 Depth-averaged peak neap ebb (top panel) and peak neap flood (bottom panel) tidal currents in the vicinity of the Marina Site. Bathymetry representative of conditions prior to the development of the Opua Marina.

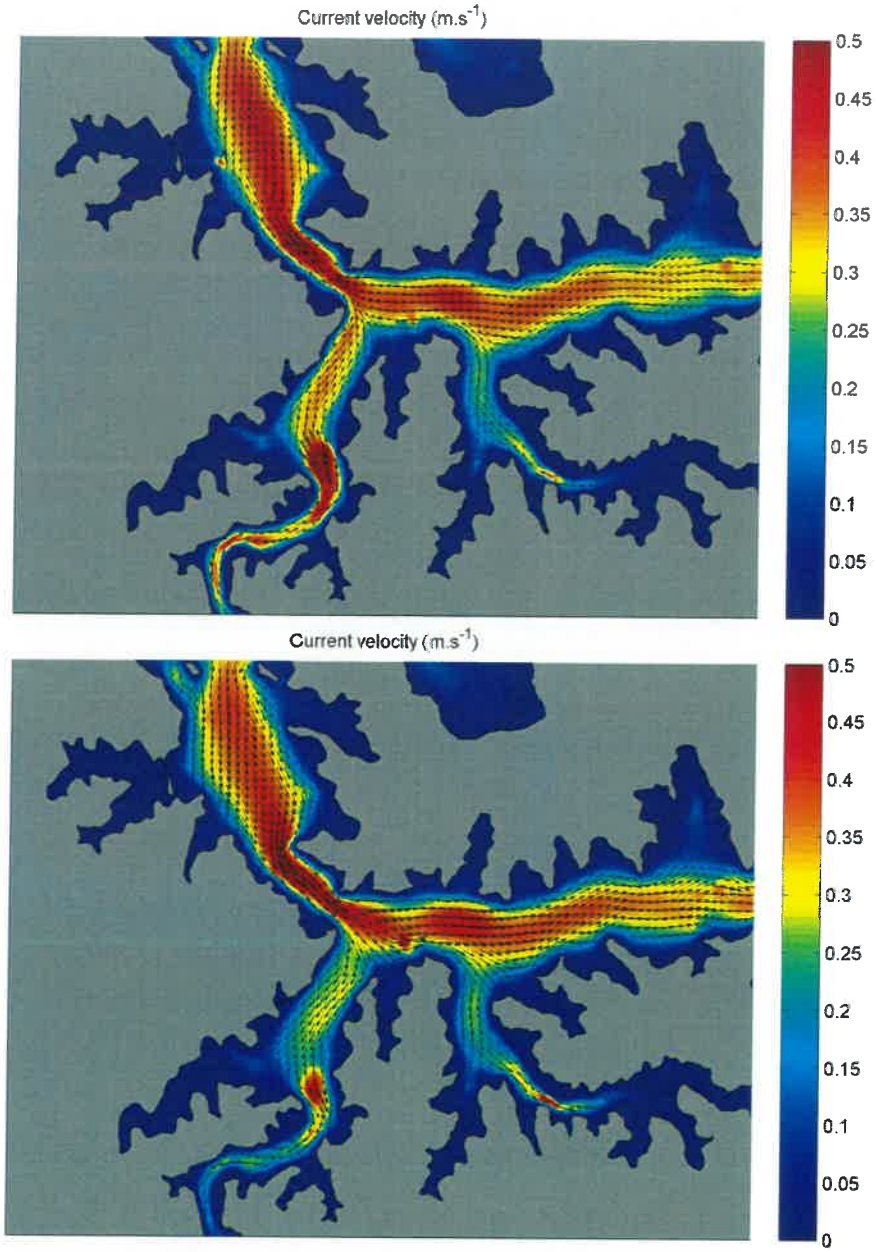

Figure 6.3 Broad scale depth-averaged peak spring ebb (top panel) and peak spring flood (bottom panel) tidal currents. Bathymetry representative of conditions prior to the development of the Opua Marina.

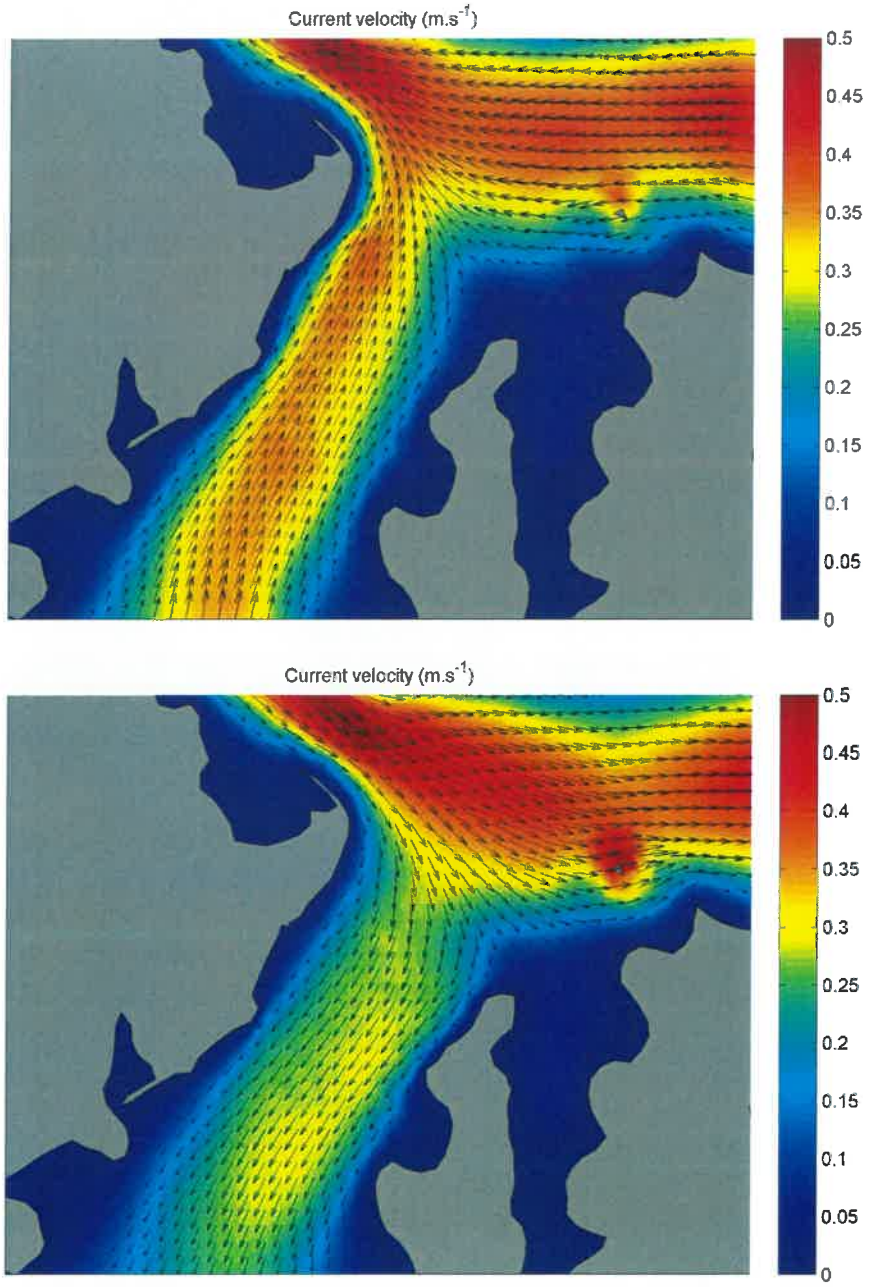

Figure 6.4 Depth-averaged peak spring ebb (top panel) and spring flood (bottom panel) tidal currents in the vicinity of the Marina Site. Bathymetry representative of conditions prior to the development of the Opua Marina.

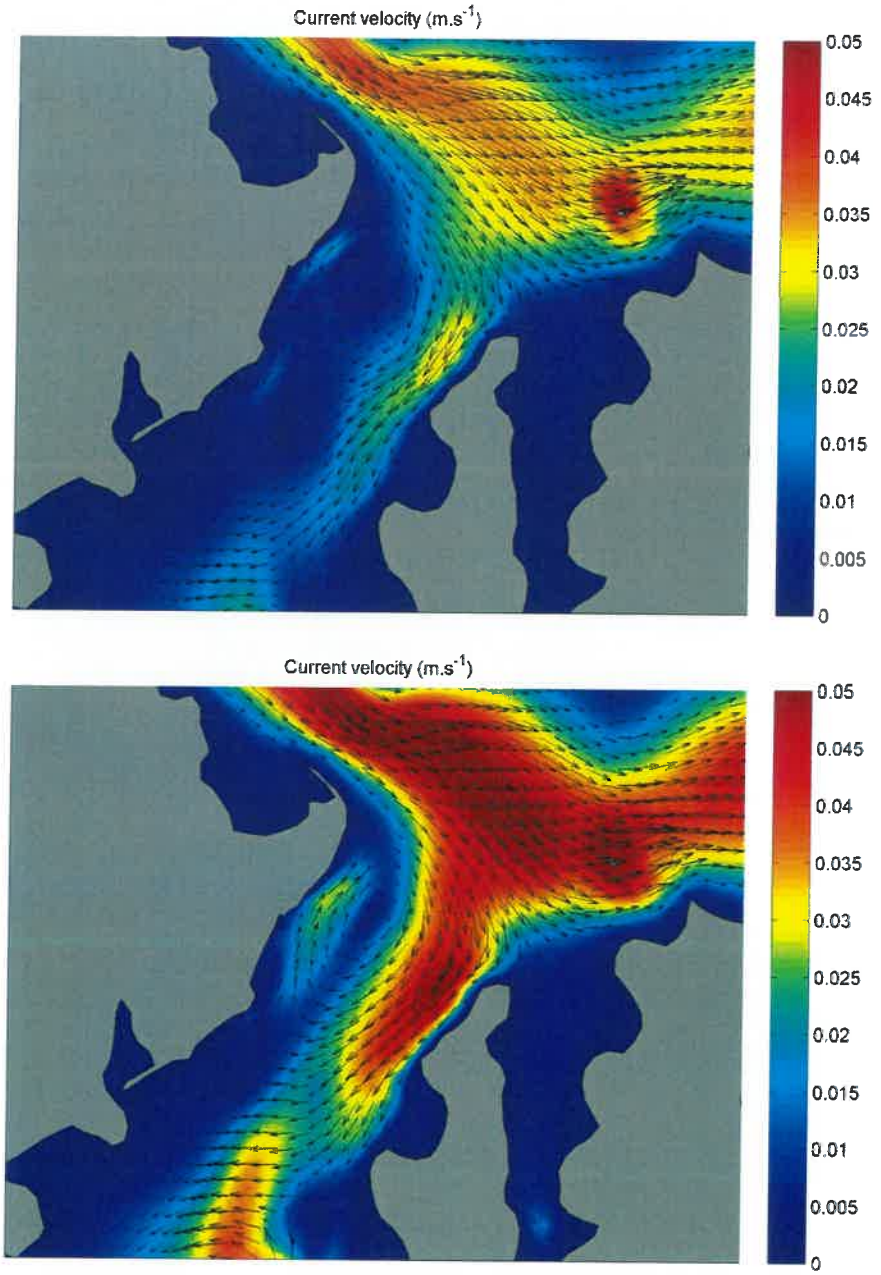

Figure 6.5 Net current over a neap tidal cycle (top panel) and spring tidal cycle (bottom panel) in the vicinity of the Marina site. Bathymetry representative of conditions prior to the development of the Opua Marina.

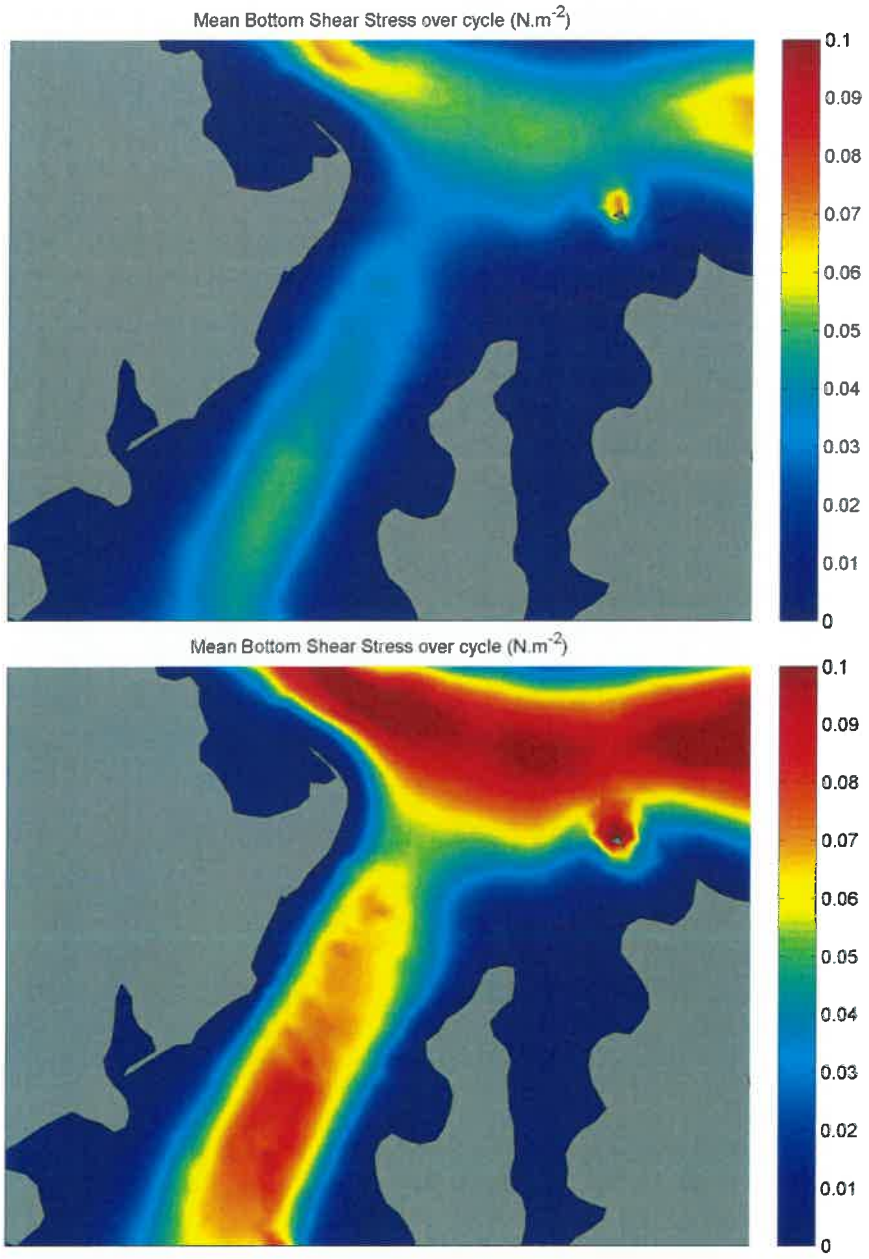

Figure 6.6 Predicted mean bed shear stress over a neap tidal cycle (top panel) and spring tidal cycle (bottom panel) in the vicinity of the Marina site. Bathymetry representative of conditions prior to the development of the Opua Marina.

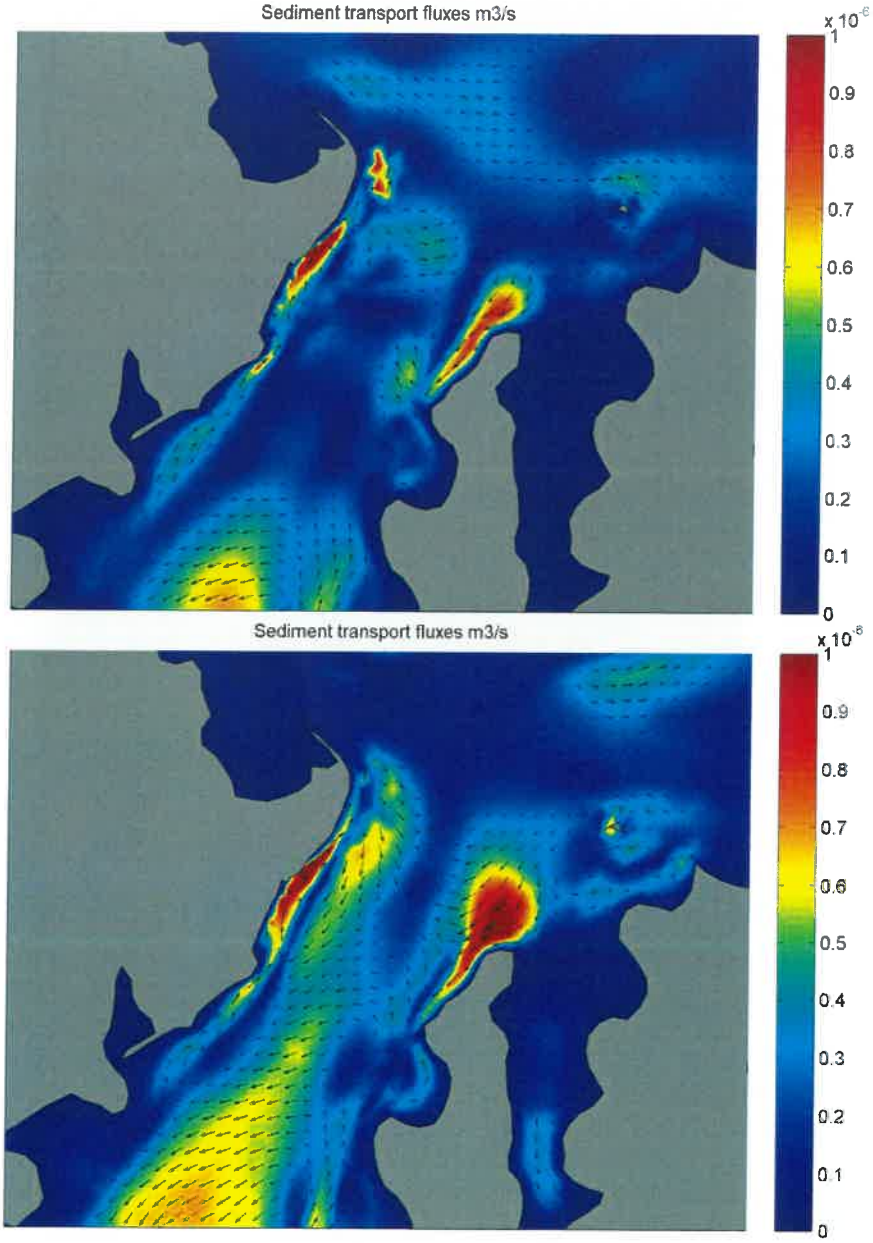

Figure 6.7 Predicted sediment transport capacity over a neap tidal cycle (top panel) and spring tidal cycle (bottom panel) in the vicinity of the Marina site. Bathymetry representative of conditions prior to the development of the Opua Marina.

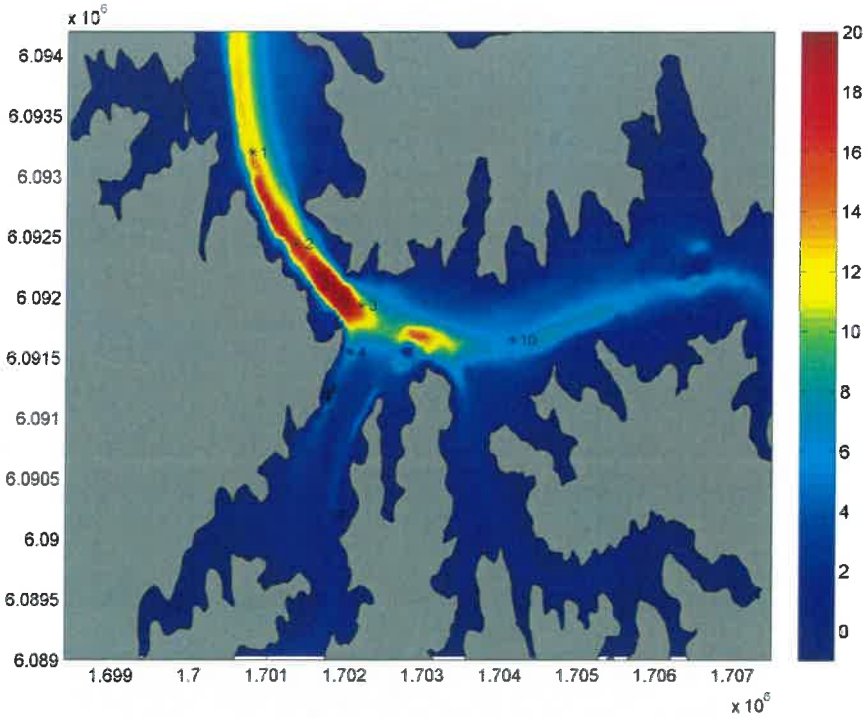

Figure 6.8 Location of sites used for time-series sites (Appendix 1). Note that the bathymetry is for the pre Marina conditions.

6.2. Hydrodynamics - Stage 1

The following section of the report gives an overview of the results from the hydrodynamic model run with bathymetry representing the existing Marina. Results are presented in terms of both model predictions for the existing Marina and changes relative to pre Marina conditions.

Small changes in peak ebb flows occur across the width of the Kawakawa River (Figure 6.9) due to the existing Marina. Maximum increases in peak neap ebb flows of 0.05 $m.s^{-1}$ occur along the inshore section south of the Marina, with maximum decreases in peak neap ebb flows of 0.05 $m.s^{-1}$ occurring within the southern sector of the existing Marina. At peak neap flood flows (Figure 6.10) changes of less than +/- 0.02 $m.s^{-1}$ are expected across the width of the Kawakawa River.

Relative to the pre-marina stage, increased peak spring ebb flows of 0.05 $m.s^{-1}$ are expected along the inshore area of the Marina (Figure 6.11) and the inshore zone south of the Marina. Maximum decreases in peak spring ebb flows of 0.03 $m.s^{-1}$ occur within the southern sector of the Marina. For peak spring flood flows (Figure 6.12) maximum increases of 0.03 $m.s^{-1}$ occur along the inshore zone south of the Marina and the western extent of the Kawakawa River. Smaller changes occur across the width of the Kawakawa River.

The mean speed at the ten time-series sites (Table 6.1), the mean difference and the distribution of changes in flow between predictions pre and post marina development are given in Table 6.2.

The predicted net current for neap tides is shown in Figure 6.13. Compared to the net currents prior to the development of the Marina (Figure 6.5) the residual flow is strengthened offshore of the Marina with an offsetting reduction in net current within the western channel and central section of the Kawakawa River.

The net current under spring tides is given in Figure 6.14. Compared to the net currents prior to the development of the Marina (Fig. 5.5) the strength of the residual current velocity along the inshore area of the Marina is reduced, with increases in residuals within the western channel and mid-section of the Kawakawa River.

Under neap tides decreases in mean bed shear over a tidal cycle (Figure 6.15) occur within the southern sector of the Marina. South of the Marina the mean bed shear stress increases in the mid-section of the Kawakawa River. Under spring tides the mean bed shear stress over the tidal cycle is decrease in the southern sector of the Marina with increases predicted to occur south of the Marina (Figure 6.16).

Overall the changes in flows and bed shear stress lead to very little change in sediment transport capacity under neap tides (Figure 6.17). A zone of increased sediment transport capacity occurs along the inshore zone of the Marina and just to the south of the Marina. South of the Marina area sediment transport rates are predicted to be reduced. Under spring tides (Figure 6.18) maximum decreases in sediment transport capacity occur along the inshore zone south of the Marina.

Actual sediment transport capacity rates in this inshore zone are relatively high (Figure 6.19) consistent with the fact that no measurable change in bed level has occur in this area (Figure 2.3). Also of note is that the area where the maximum observed deposition has occurred (towards to northern end of the Marina (Figure 2.3) corresponds to an area of divergence in sediment transport capacity.

Table 6.2 Mean speed at time-series sites (Figure 6.33) for existing Marina, mean difference in speed compared to pre Marina conditions and distribution of differences over the full one-month simulation.

	Mean Speed (m/s)	Mean Speed Difference (m/s)	Range of speed change (Existing Marina- Pre Marina)						
			<-0.035	-0.035 -0.025	-0.025 -0.015	-0.015 -0.005	-0.005 0.005	0.005 0.015	>0.015
Site1	0.210	<0.001	0.0%	0.0%	0.0%	59.7%	40.3%	0.0%	0.0%
Site2	0.124	-0.001	0.0%	0.0%	0.0%	20.3%	79.7%	0.0%	0.0%
Site3	0.123	-0.013	8.4%	23.9%	23.8%	26.1%	17.7%	0.3%	0.0%
Site4	0.098	+0.001	0.0%	0.0%	0.0%	30.3%	69.6%	0.1%	0.0%
Site5	0.124	-0.002	0.0%	0.0%	0.0%	88.3%	11.7%	0.0%	0.0%
Site6	0.134	+0.003	0.0%	0.0%	0.6%	26.1%	62.0%	11.0%	0.3%
Site7	0.159	+0.004	0.0%	0.0%	0.0%	3.7%	88.8%	5.9%	1.5%
Site8	0.047	<0.001	0.0%	0.0%	0.0%	65.5%	34.4%	0.1%	0.0%
Site9	0.077	+0.006	0.0%	0.0%	0.3%	19.5%	46.9%	22.9%	10.5%
Site10	0.085	+0.001	0.0%	0.0%	0.0%	10.3%	89.6%	0.1%	0.0%

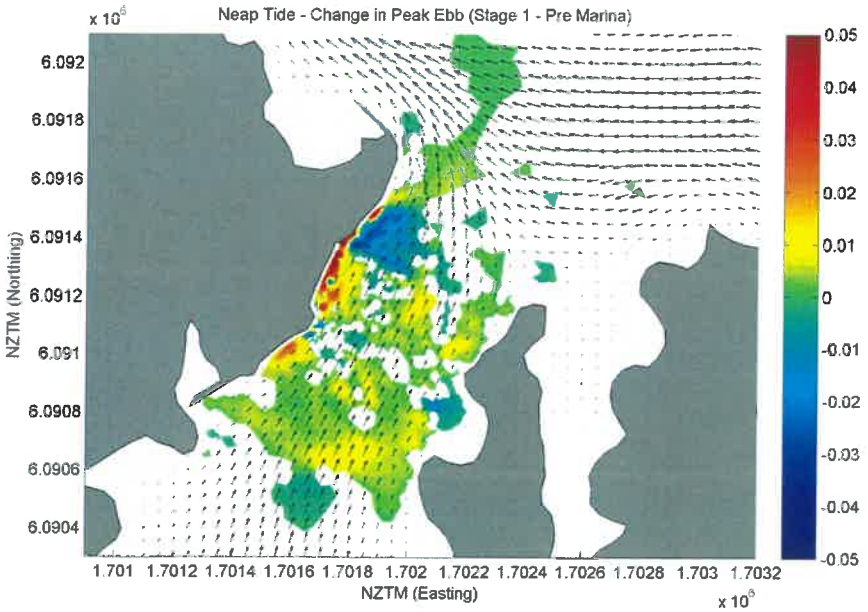

Figure 6.9 Predicted peak neap ebb tide currents and change relative to predictions with existing Marina. Area of change <0.001 not shaded. Positive change indicates predictions with Stage 1 development increase compared to pre Marina predictions.

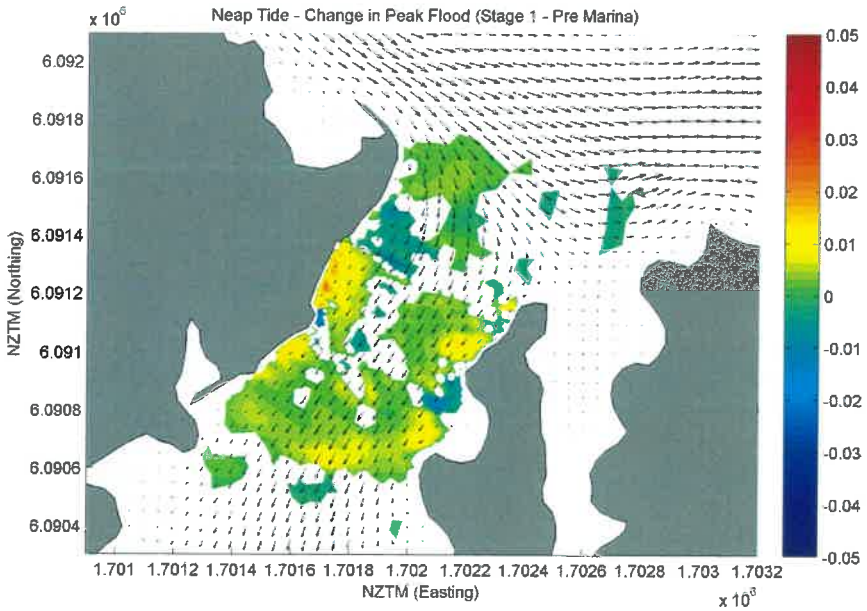

Figure 6.10 Predicted peak neap flood tide currents and change relative to predictions with existing Marina. Area of change <0.001 not shaded. Positive change indicates predictions with Stage 1 development increase compared to pre Marina predictions.

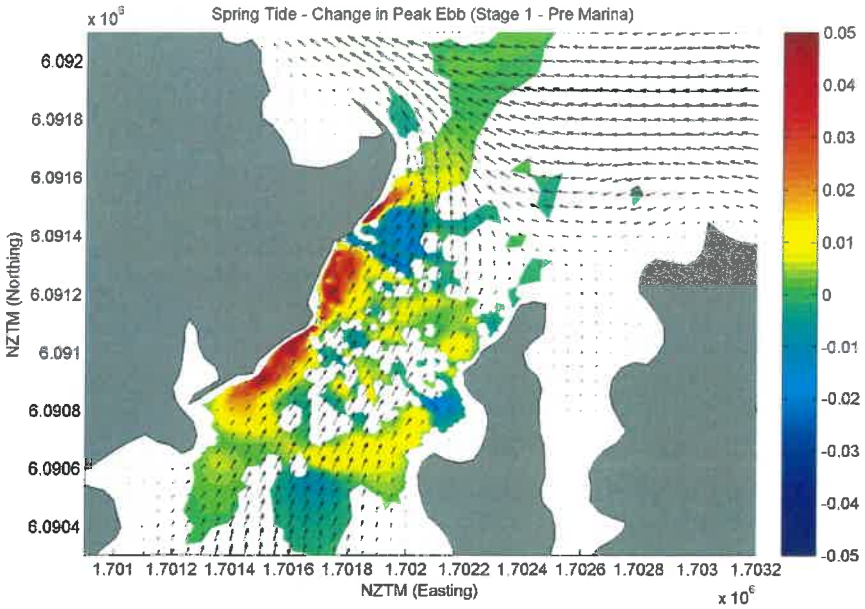

Figure 6.11 Predicted peak spring ebb tide currents and change relative to predictions with existing Marina. Area of change <0.001 not shaded. Positive change indicates predictions with Stage 1 development increase compared to pre Marina predictions.

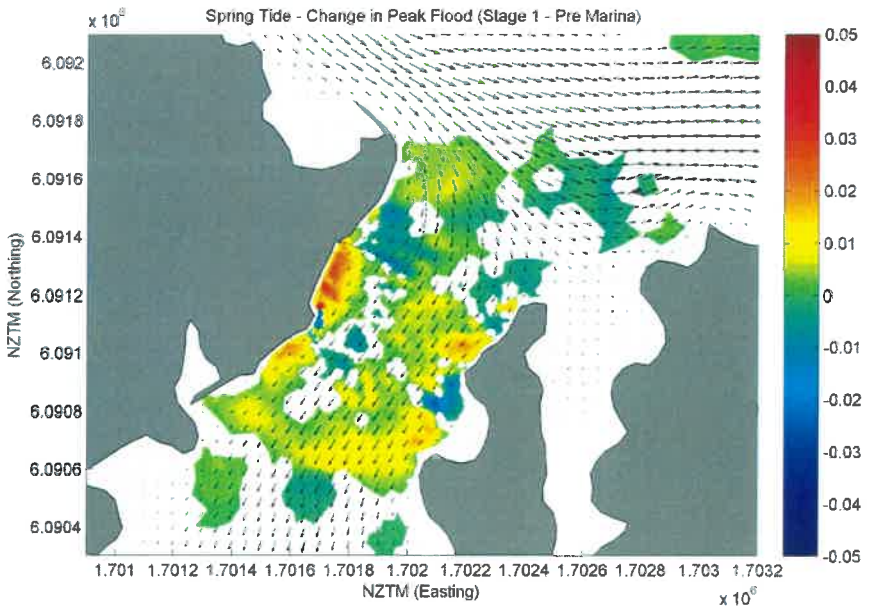

Figure 6.12 Predicted peak spring flood tide currents and change relative to predictions with existing Marina. Area of change <0.001 not shaded. Positive change indicates predictions with Stage 1 development increase compared to pre Opua Marina predictions.

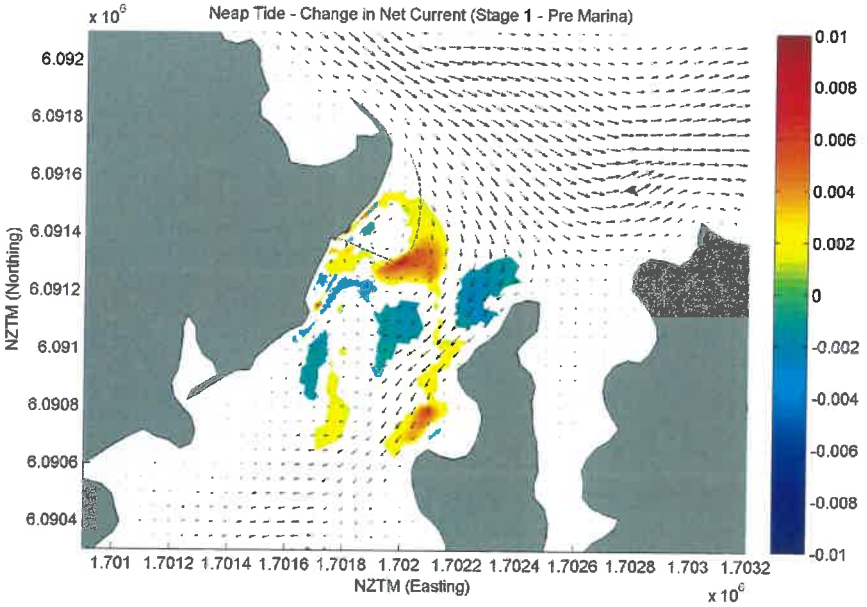

Figure 6.13 Predicted residual current under neap tide and change relative to predictions with existing Marina. Area of change <0.001 not shaded. Positive change indicates predictions with Stage 1 development increase compared to pre Opua Marina predictions.

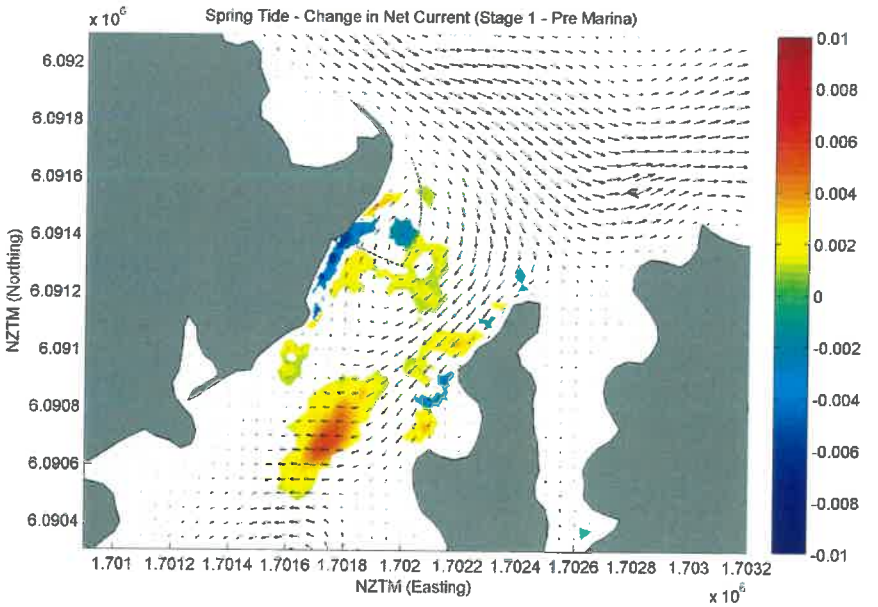

Figure 6.14 Predicted residual current under spring tide and change relative to predictions with existing Marina. Area of change <0.001 not shaded. Positive change indicates predictions with Stage 1 development increase compared to pre Opua Marina predictions.

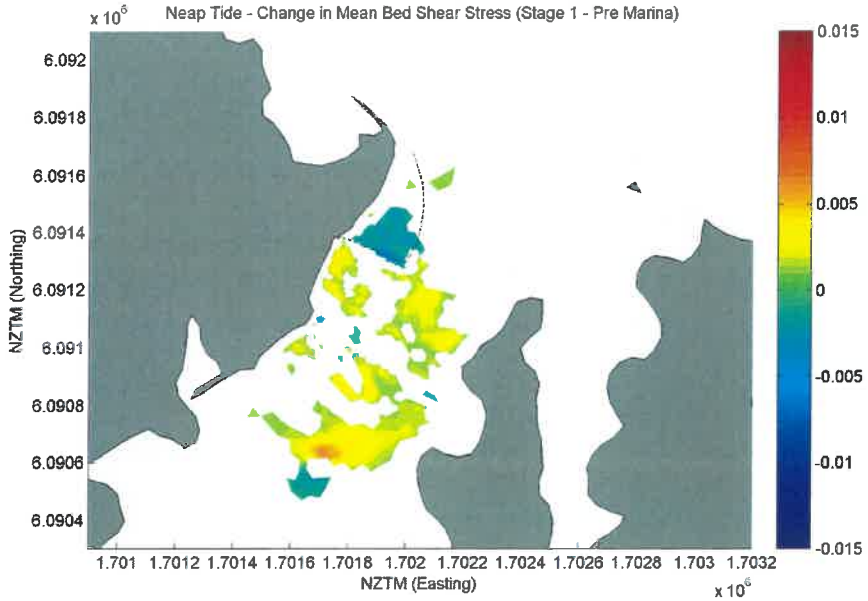

Figure 6.15 Change in mean bed shear stress under neap tide relative to predictions with existing Marina. Area of change <0.001 not shaded. Positive change indicates predictions with Stage 1 development increase compared to pre Opua Marina predictions.

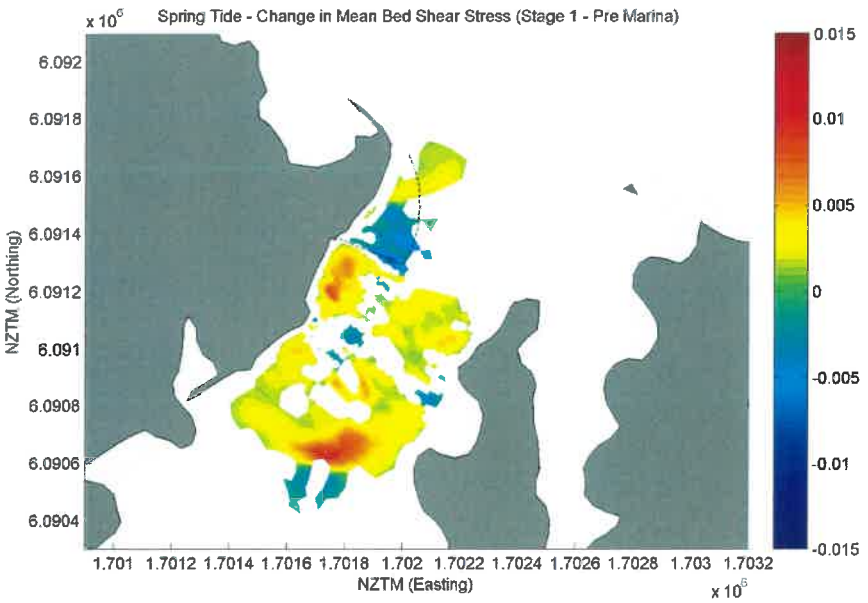

Figure 6.16 Change in mean bed shear stress under spring tide relative to predictions with existing Marina. Area of change <0.001 not shaded. Positive change indicates predictions with Stage 1 development increase compared to pre Opua Marina predictions.

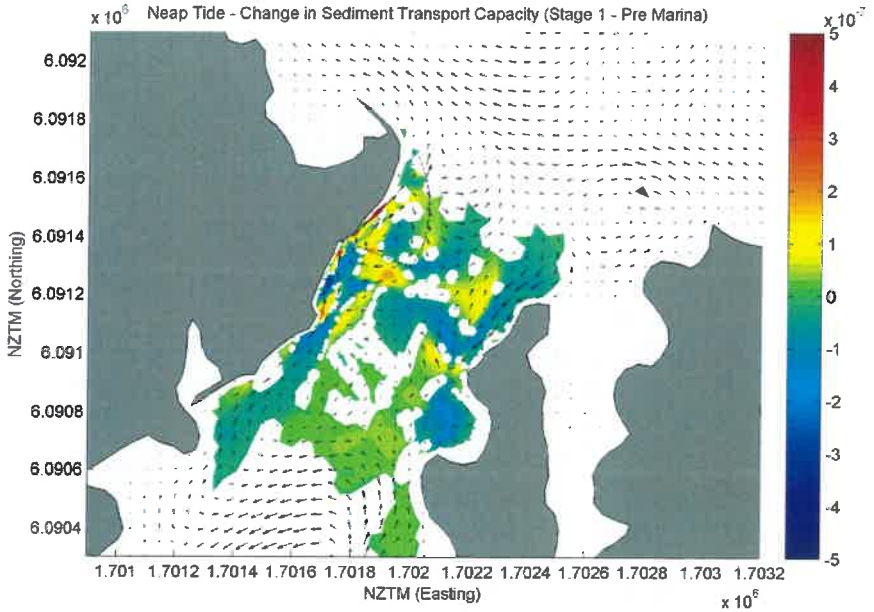

Figure 6.17 Predicted sediment transport capacity under neap tide and change relative to predictions with existing Marina. Area of change $<10^{-8}$ not shaded. Positive change indicates predictions with Stage 1 development increase compared to pre Opua Marina predictions.

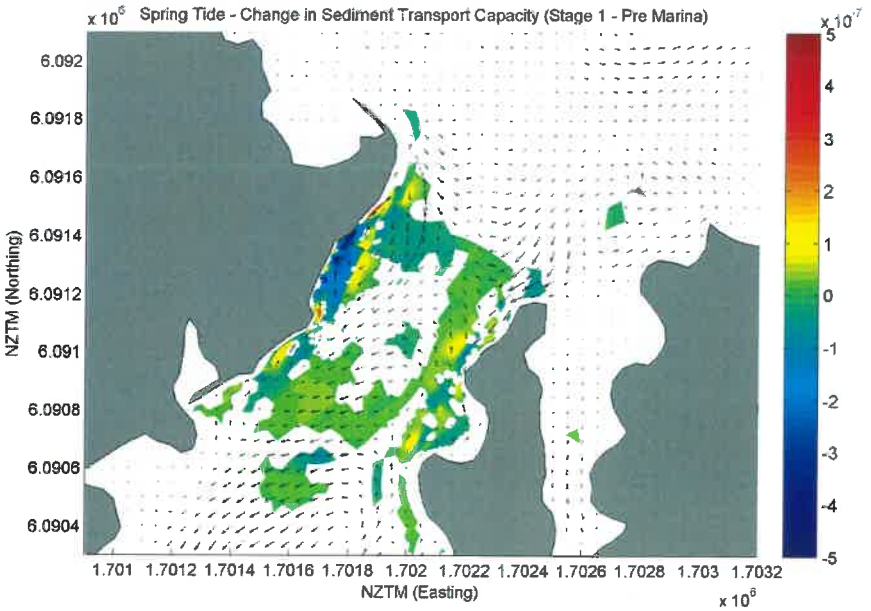

Figure 6.18 Predicted sediment transport capacity under spring tide and change relative to predictions with existing Marina. Area of change $<10^{-8}$ not shaded. Positive change indicates predictions with Stage 1 development increase compared to pre Opua Marina predictions.

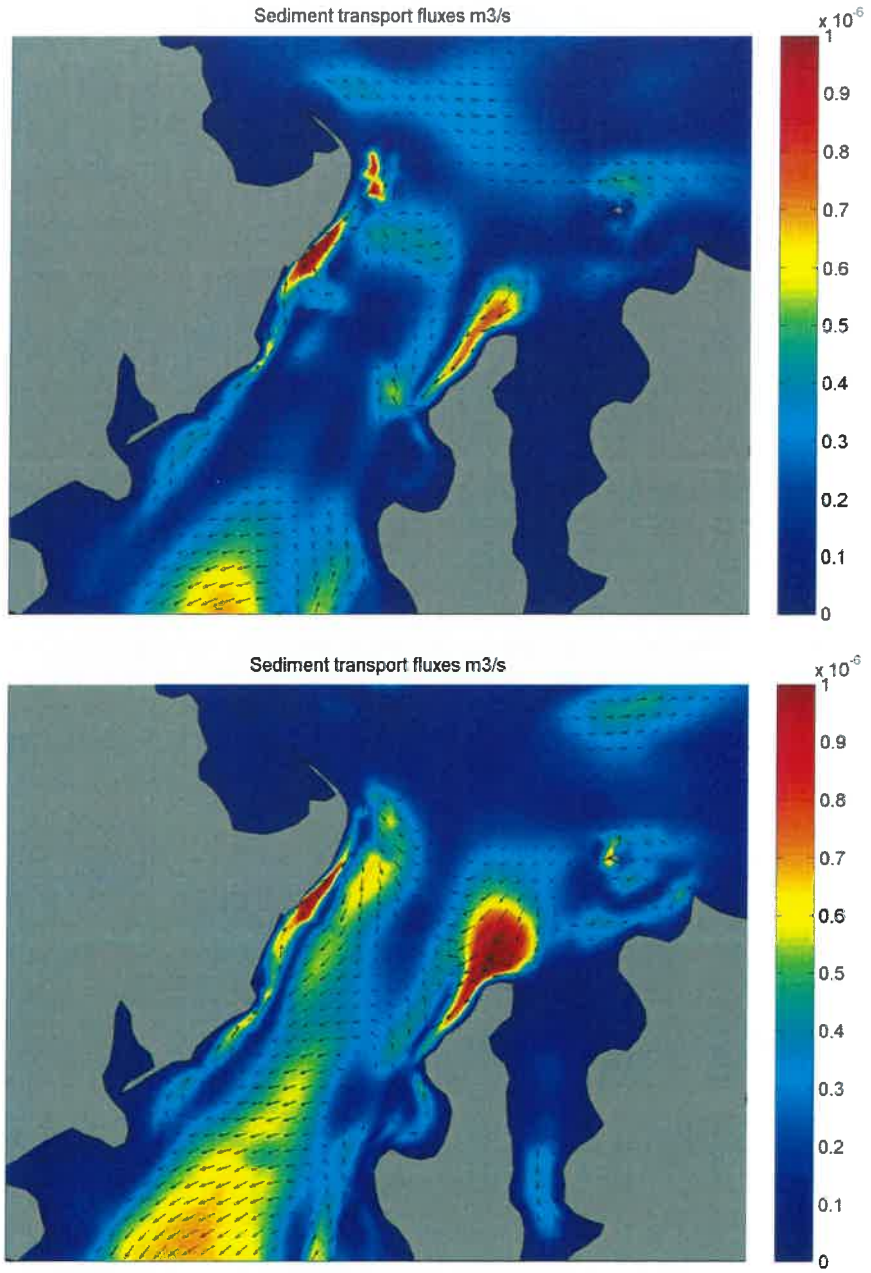

Figure 6.19 Predicted sediment transport capacity over a neap tidal cycle (top panel) and spring tidal cycle (bottom panel) in the vicinity of the Marina site. Bathymetry representative of conditions with Stage 1 Marina.

6.3. Hydrodynamics - Stage 2

The following section of the report provides an overview of the results from the hydrodynamic model run with bathymetry representing the proposed Stage 2 development. Results are presented in terms of both model predictions with the Stage 2 development in place and changes relative to existing Marina predictions.

Maximum decreases in peak neap ebb flows occur within the inshore sector of the Marina (Figure 6.20) with smaller decreases occurring offshore of the marina. Increases in peak neap ebb flows occur within the western channel of the Kawakawa River. The maximum decrease in peak neap flood flows (Figure 6.21) occurs within the Marina, with smaller decreases within the eastern channel of the Kawakawa River.

Increases in peak spring ebb flows of 0.02 $m.s^{-1}$ are predicted to occur within the southern sector of the existing Marina (Figure 6.22). Maximum decreases in peak spring ebb flows of 0.05 $m.s^{-1}$ occur within the Stage 2 Marina with smaller decreases offshore of the Marina. A similar pattern of decrease is predicted to occur for peak spring flood flows (Figure 6.23)

The distribution of changes in flow between predictions pre and post marina development at the ten time-series sites (Table 6.1) are given in Table 6.2.

The predicted net current for neap tides is shown in Figure 6.24. Compared to the net currents with the existing Marina in place (Figure 6.13) the north-easterly directed residual flow within the south-west corner of the existing Marina is significantly reduced in strength. Similarly the net current within the Kawakawa River is reduced by around 0.006 $m.s^{-1}$. The net current under spring tidal conditions is given in Figure 6.25. Compared to the net currents prior to the development of the Marina (Figure 6.5) residual flows are decreased in the area offshore of the Marina and within the existing Marina. Small increases in residual flows are predicted to occur within the southern sector of the Marina.

Under neap tides a decrease in mean bed shear over a tidal cycle is predicted to occur within the area of the proposed dredging (Figure 6.26). Under spring tides there are two areas where the mean bed shear stress over the tidal cycle increases (Figure 6.27) – just outside the north-east and north-west corner of the Marina. Within, and just offshore of the proposed marina area, mean bed shear stress decreases.

Overall the changes in flows and bed shear stress lead to small changes in sediment transport capacity under neap tides (Figure 6.28). A decrease in sediment transport capacity is predicted to occur within the inshore zone of the Marina and a zone of increased sediment transport capacity occurs towards the southern area of the marina and within the eastern channel of the Kawakawa River.

Under spring tides (Figure 6.29) a decrease in sediment transport capacity occurs along the inshore edge of the proposed dredge area and into the existing Marina. Just offshore from this zone there is an area of increased sediment transport capacity.

Actual sediment transport capacity rates are relatively high in the existing Marina area (Figure 6.30) so the predicted decrease in sediment transport capacity is unlikely to lead to increased deposition in this area. The reductions in sediment transport capacity rates along the inshore zone and in the lee of the Stage 2 Marina indicate that the deposition of catchment derived sediments may occur within these areas. The actual rate of deposition will depend on the quantity of catchment derived sediment arriving within the Marina – this is discussed in Section 6.5.

Table 6.3 Mean speed at time-series sites (Figure 6.33) for Stage 2 development, mean difference in speed compared to existing Marina conditions and distribution of differences over the full one-month simulation.

	Mean Speed (m/s)	Difference in Mean Speed (m/s)	Range of speed change (Sage 2 Marina - Existing Marina)						
			<-0.025	-0.025 -0.015	-0.015 -0.005	-0.005 0.005	0.005 0.015	0.015 0.025	>0.025
Site1	0.210	<0.001	0.0%	0.0%	34.6%	65.4%	0.0%	0.0%	0.0%
Site2	0.126	+0.003	0.0%	0.0%	1.9%	98.0%	0.1%	0.0%	0.0%
Site3	0.137	+0.001	0.5%	7.5%	44.5%	40.4%	7.0%	0.0%	0.0%
Site4	0.099	+0.002	0.0%	0.0%	12.2%	87.7%	0.1%	0.0%	0.0%
Site5	0.125	-0.001	0.0%	0.0%	98.7%	1.3%	0.0%	0.0%	0.0%
Site6	0.137	+0.006	0.0%	0.3%	4.4%	80.8%	13.5%	1.1%	0.0%
Site7	0.160	+0.005	0.0%	0.0%	2.5%	87.7%	8.3%	1.3%	0.2%
Site8	0.045	+0.002	0.0%	0.0%	96.3%	3.7%	0.0%	0.0%	0.0%
Site9	0.074	-0.005	0.0%	0.0%	5.8%	87.6%	6.6%	0.0%	0.0%
Site10	0.085	+0.001	0.0%	0.0%	13.5%	86.5%	0.1%	0.0%	0.0%

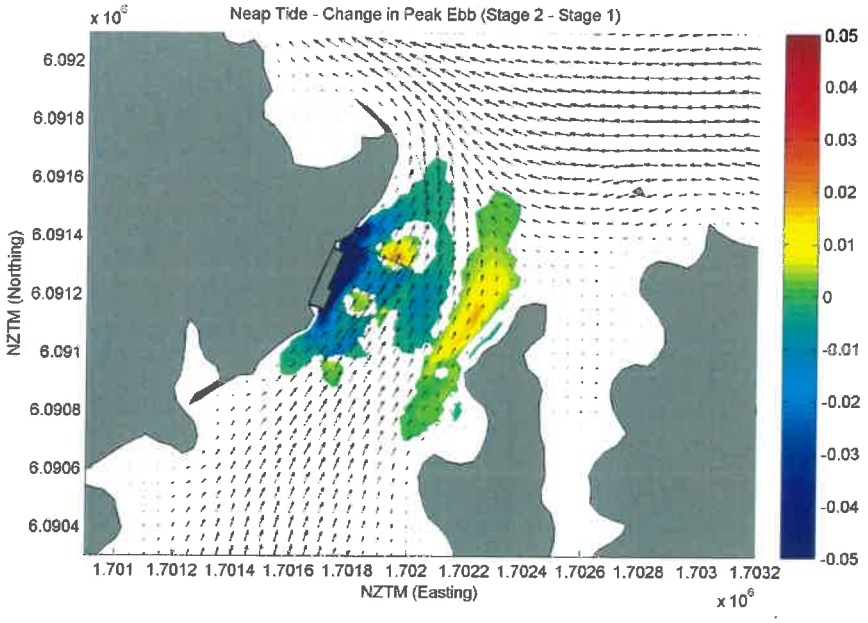

Figure 6.20 Predicted peak neap ebb tide currents and change relative to predictions with existing Marina. Area of change <0.001 not shaded. Positive change indicates predictions with Stage 2 development increase compared to existing Marina predictions.

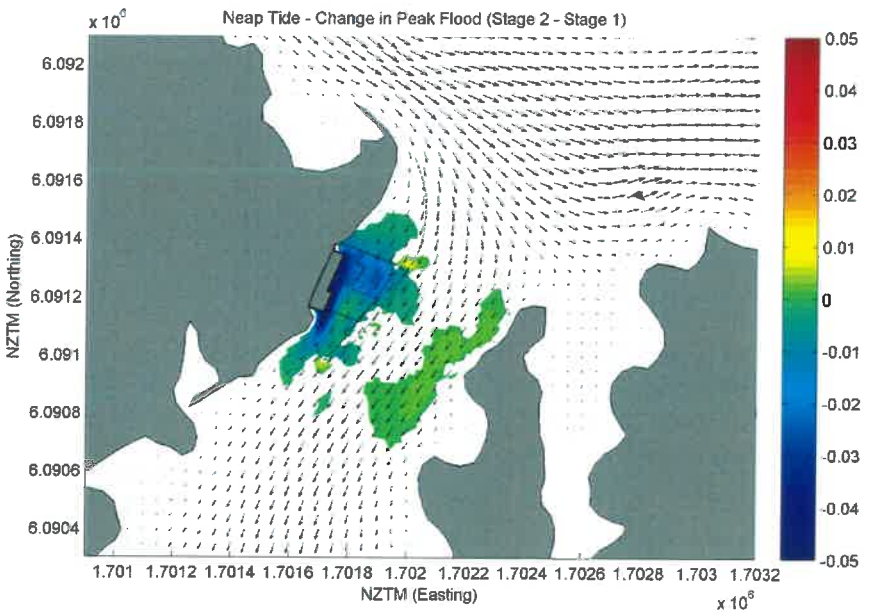

Figure 6.21 Predicted peak neap flood tide currents and change relative to predictions with existing Marina. Area of change <0.001 not shaded. Positive change indicates predictions with Stage 2 development increase compared to existing Marina predictions.

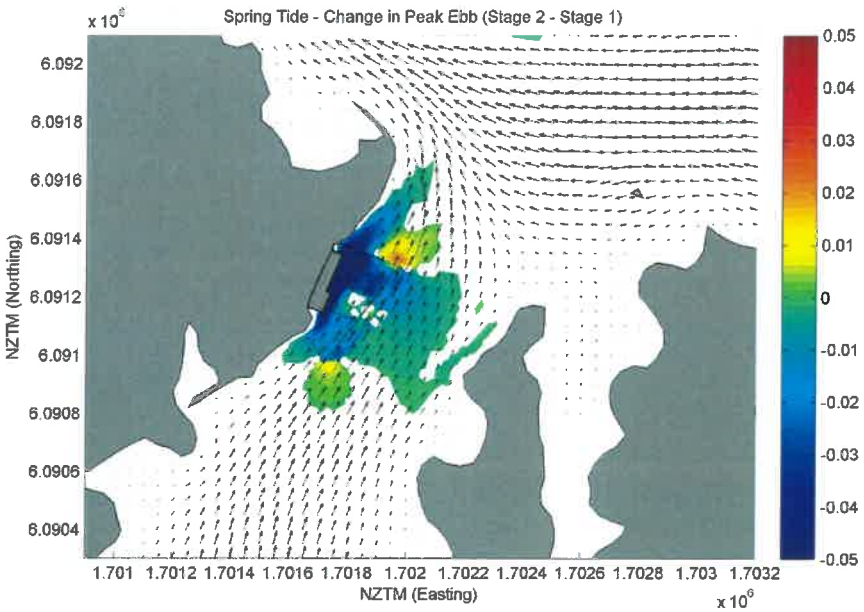

Figure 6.22 Predicted peak spring ebb tide currents and change relative to predictions with existing Marina. Area of change <0.001 not shaded. Positive change indicates predictions with Stage 2 development increase compared to existing Marina predictions.

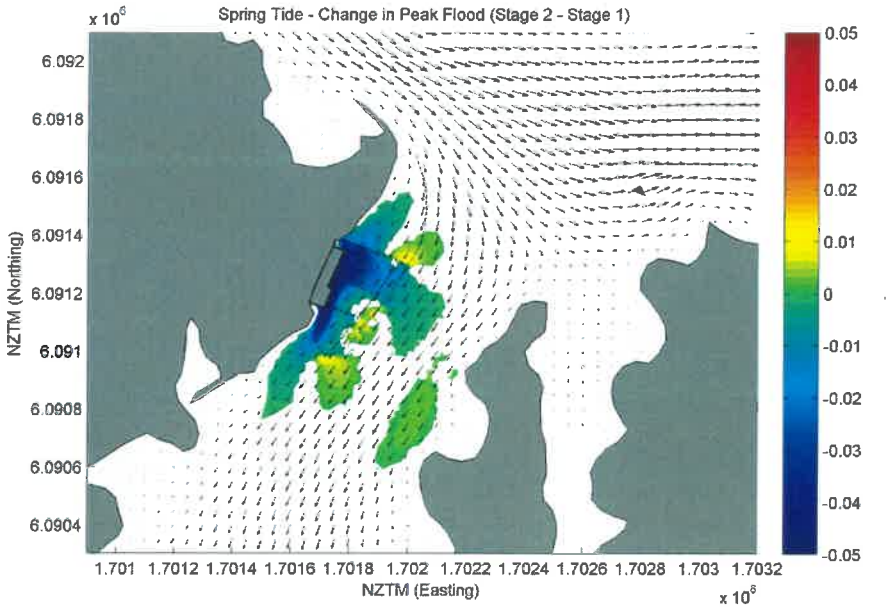

Figure 6.23 Predicted peak spring flood tide currents and change relative to predictions with existing Marina. Area of change <0.001 not shaded. Positive change indicates predictions with Stage 2 development increase compared to existing Marina predictions.

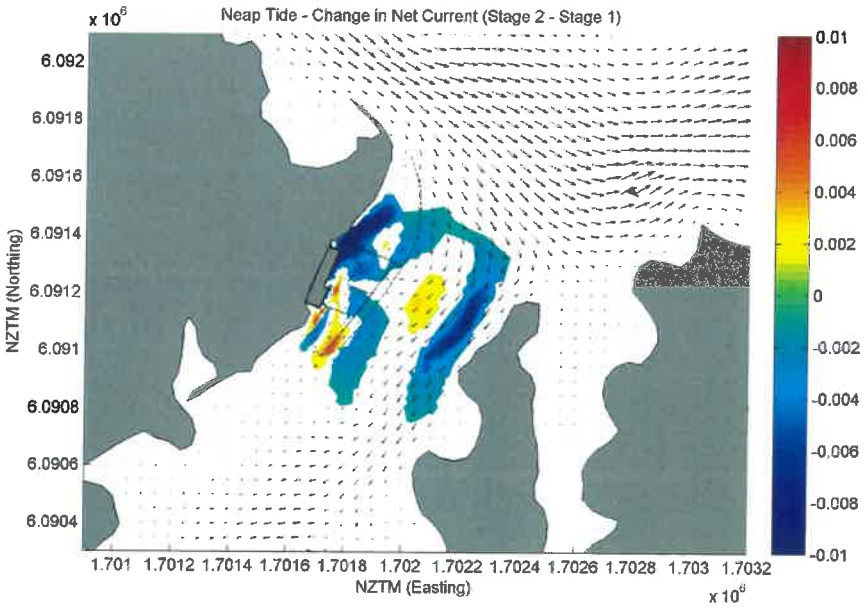

Figure 6.24 Predicted residual current under neap tide and change relative to predictions with existing Marina. Area of change <0.001 not shaded. Positive change indicates predictions with Stage 2 development increase compared to existing Marina predictions.

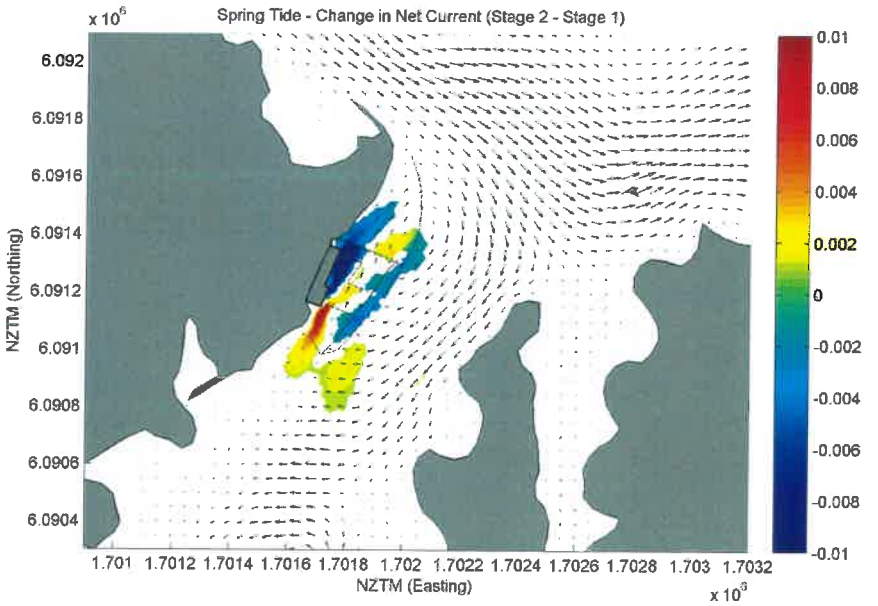

Figure 6.25 Predicted residual current under spring tide and change relative to predictions with existing Marina. Area of change <0.001 not shaded. Positive change indicates predictions with Stage 2 development increase compared to existing Marina predictions.

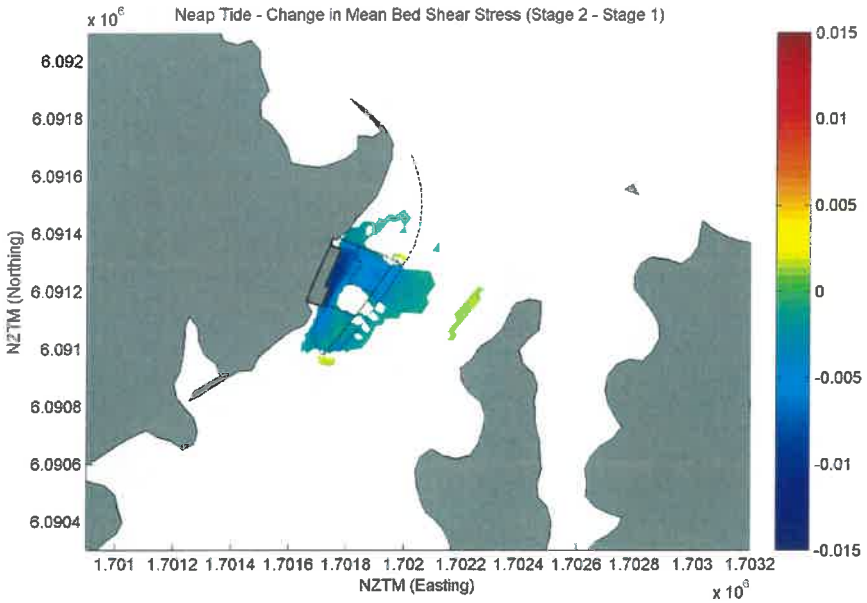

Figure 6.26 Change in mean bed shear stress under neap tide relative to predictions with existing Marina. Area of change <0.001 not shaded. Positive change indicates predictions with Stage 2 development increase compared to existing Marina predictions.

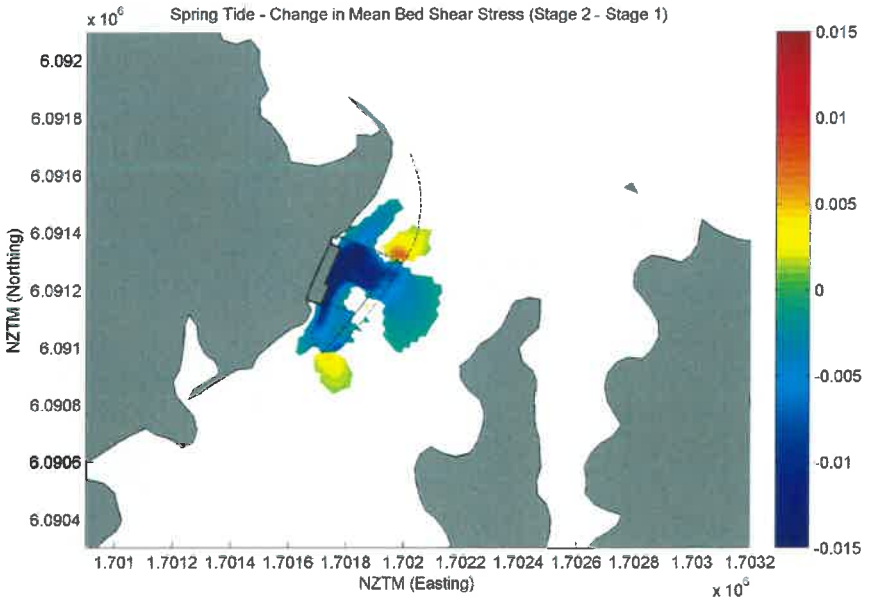

Figure 6.27 Change in mean bed shear stress under spring tide relative to predictions with existing Marina. Area of change <0.001 not shaded. Positive change indicates predictions with Stage 2 development increase compared to existing Marina predictions.

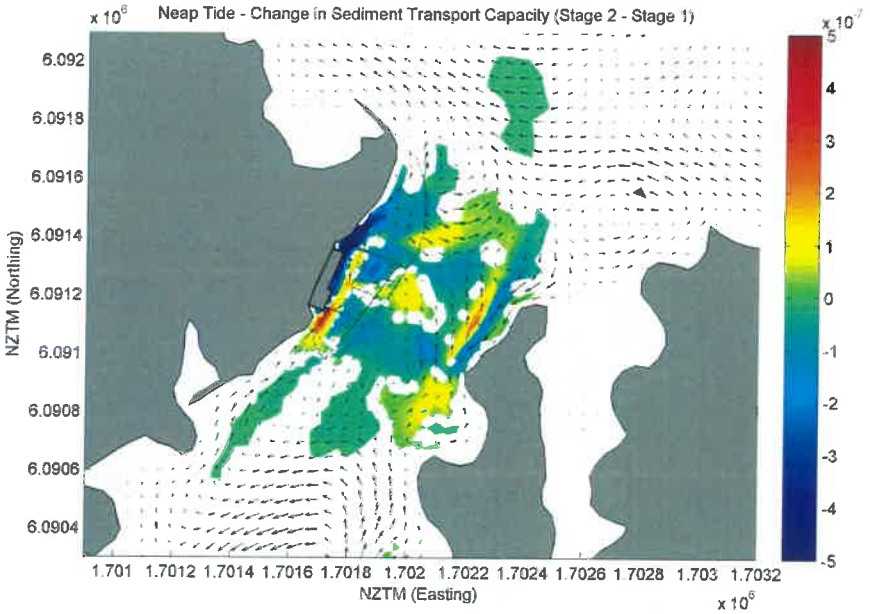

Figure 6.28 Predicted sediment transport capacity under neap tide and change relative to predictions with existing Marina. Area of change $<10^{-8}$ not shaded. Positive change indicates predictions with Stage 2 development increase compared to existing Marina predictions.

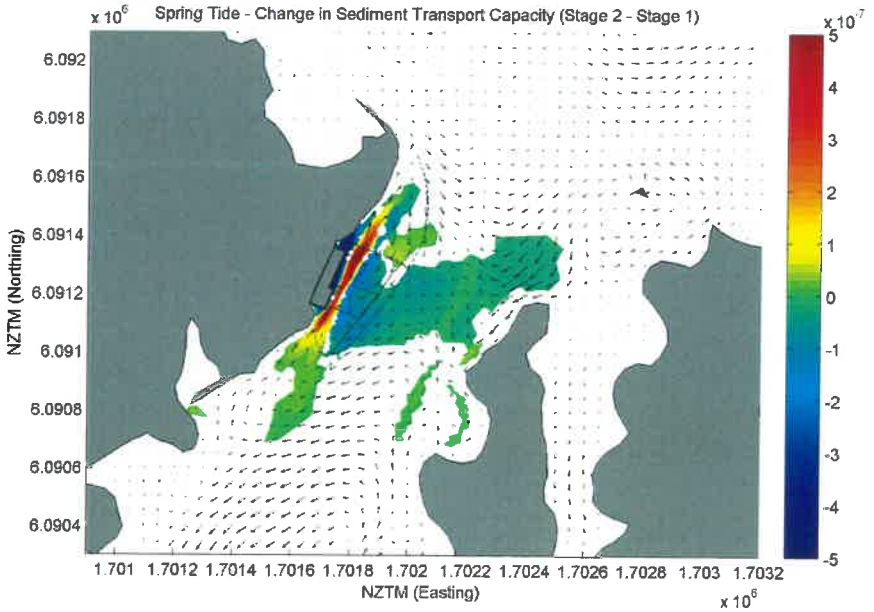

Figure 6.29 Predicted sediment transport capacity under spring tide and change relative to predictions with existing Marina. Area of change $<10^{-8}$ not shaded. Positive change indicates predictions with Stage 2 development increase compared to existing Marina predictions.

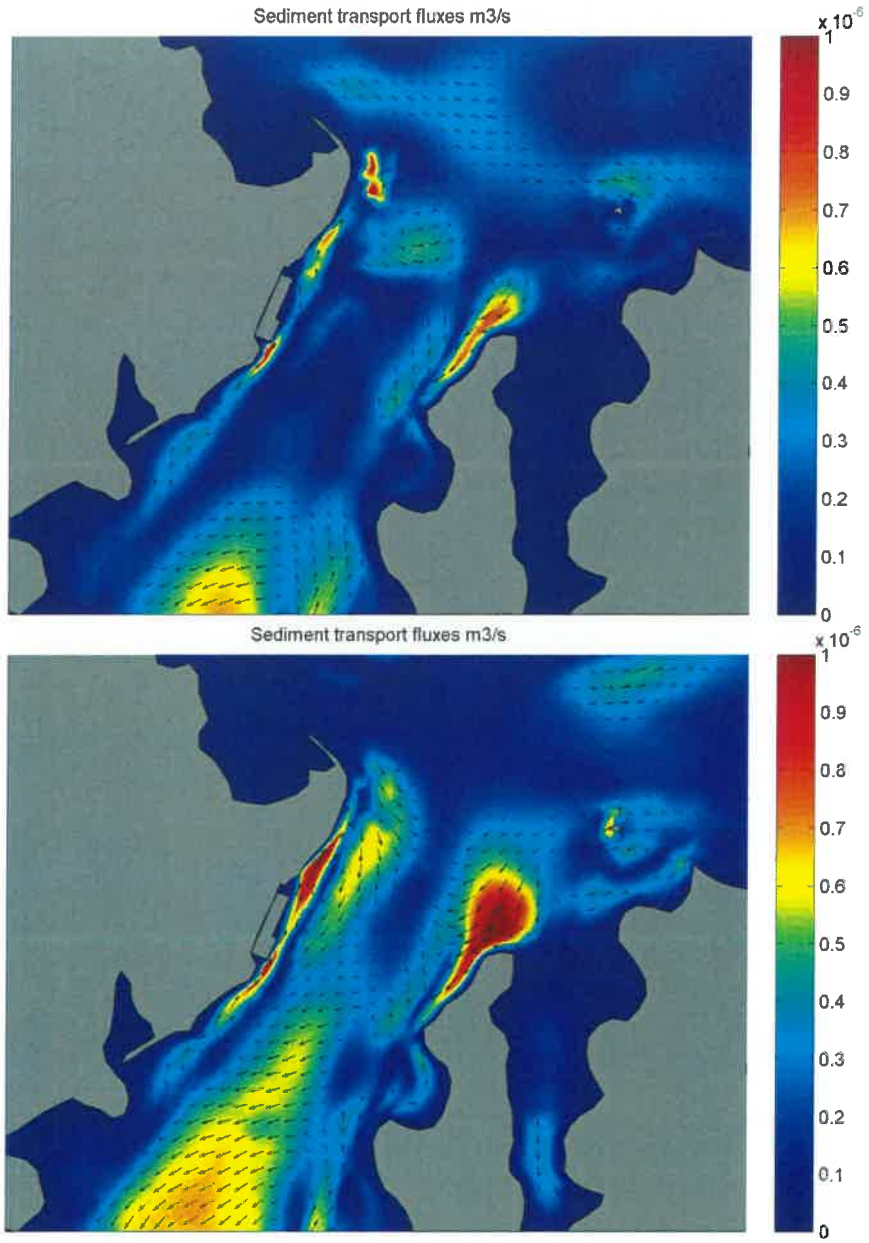

Figure 6.30 Predicted sediment transport capacity over a neap tidal cycle (top panel) and spring tidal cycle (bottom panel) with the Stage 2 Marina development.

6.4. Marina contaminant pathways

In this section of the report results from Ptrack simulations are presented for a generic contaminant plume emanating from the area of the Stage 2 development. The contaminant is assumed to be conservative so no decay processes, settlement or chemical decomposition are modelled. Model results therefore provide an upper bound in terms of the likely plume extent and dilutions achieved.

The release scenario modelled consisted of a continuous release of particles from within the Stage 2 area over a five-day period (starting on both a spring and neap tide). Such a release scenario is not realistic in terms of the management if the Marina. Actual effects of contaminants will be dependent on the length of release, timing of release relative to state of tide, non-conservative contaminant behaviour and location of release within the Marina. However, model results provide a probabilistic quantification of the physical mixing of Marina contaminants within the Kawakawa River, Waikare Inlet and Veronica Channel and provide quantification of the envelope of the potential effects of Marina contaminants.

Using the variable kernel technique outlined in Section 3.2 the predicted location of the particles at each half-hour time-step during the five-day simulation were used to define the mean depth-averaged concentration map for the spring and neap simulations (Figure 6.31 and Figure 6.32 respectively). Model results are presented in terms of relative concentration with a source concentration defined as a value of 1. Results are therefore scalable for any given source concentration.

The area of highest mean concentration occur in the narrow band inshore of the Marina and towards the Opua Wharf and Ferry Ramp. Ten-fold dilution is achieved within 1500 m south of the Marina along the western channel of the Kawakawa River. Limited dilution of contaminants occurs between the Marina, the Opua Wharf and Ferry Ramp. However along the southern shoreline of the Veronica Channel (towards English Bay) ten-fold dilution is achieved within 1300 m of the Wharf.

Predicted relative concentrations within the entrance to Waikare Inlet are less than 0.05 with rapid dilution occurring within the Inlet itself.

To further illustrate the degree of dilution that occurs and the effects that the timing of the release may have on plume dynamics time-series plots of concentrations at the key sites (Figure 6.33) for the Ptrack spring and neap simulations are shown in Figure 6.34 and Figure 6.35 respectively.

Within the Veronica channel (Sites 1-3, Figure 6.34 & Figure 6.35) peak relative concentrations of between 0.1 to 0.7 occur at low tide. During the flood tide the plume is advected back towards the marina and into the Waikare Inlet resulting in low relative concentrations at these times for these sites. The clear tidal modulation of the predicted relative concentrations at Sites 1 and 2 is less apparent at Site 3 due to the dynamics of ebb and flood tidal currents (i.e. Figure 6.4), the partitioning of flows between the eastern and western channels of the Kawakawa River and the influence of the flows into and out of the Waikare Inlet. This is

highlighted by the quite different estimates of relative concentrations at this site under the spring and neap tide simulations.

At Site 4 clear peaks in relative concentrations occur at low tide with minimum relative concentrations values occurring on the flooding tide.

Within the Marina (Site 5) the relative concentration varies as a function of total water depth and strength of current - maximum water depths occur at high water effectively reducing depth-averaged concentrations. At other times the strength of the tidal current determines how the contaminant plume is advected away from the release point and thus the predicted depth-averaged relative concentration.

At site 6 (Kawakawa River, western channel) the predicted relative concentrations are a combination of the effect of the flooding tide (advecting the plume directly away from the Marina onto this site) and the ebb tide advection of the plume that has already been transported up the Kawakawa River on the previous flood tide.

The very low relative concentrations predicted to occur at Sites 7 (Kawakawa River, eastern channel) and 8 (Waikare Inlet) indicate the high degree of dilution that occurs once the plume is transported to these areas.

6.4.1. Dredge Plume

Information from dredging operations within the Whangarei Harbour indicate that source concentrations of around 0.14 $kg.m^{-3}$ can be achieved using the dredging practice to be adopted for the Stage 2 development (M. Beazley, pers. comm. based on NRC data). Using the predicted time-series data of relative concentration and this source concentration the data in Table 6.4 can be derived to give the expected maximum and mean suspended sediment concentrations that are likely to occur during the dredging operation at the time-series sites (Figure 6.33).

Table 6.4 Maximum and mean suspended sediment concentrations at time-series sites (Figure 6.33) during dredging operation assuming a maximum source concentration of 0.14 $kg.m^{-3}$.

Time Series Site	Maximum suspended sediment concentration ($kg.m^{-3}$)	Mean suspended sediment concentration ($kg.m^{-3}$)
Site 1	0.033	0.006
Site 2	0.111	0.034
Site 3	0.070	0.007
Site 4	0.118	0.038
Site 5	0.140	0.047
Site 6	0.107	0.046
Site 7	0.014	0.004
Site 8	0.002	<0.001

The maximum values in Table 6.4 are in the lower levels of suspended sediment concentrations observed by NIWA during drought conditions (Section 2.3) within the Veronica Channel and well below the observed suspended sediment concentrations within the Waikare Inlet.

As can be seen from the time-series plots (Figure 6.33 and Figure 6.34) the duration of the peaks in suspended sediment concentration are relatively short. This results in the low estimates of mean suspended sediment concentrations shown in Table 6.4.

Also of note is the observed suspended sediment concentration for the outer instrument site (Site D4, Figure 1.1) where levels of 0.1-0.4 $kg.m^{-3}$ were recorded. This gives a good indication of the influence of sediment sources other than the Kawakawa and Waikare catchments in terms of the overall Bay of Islands system.

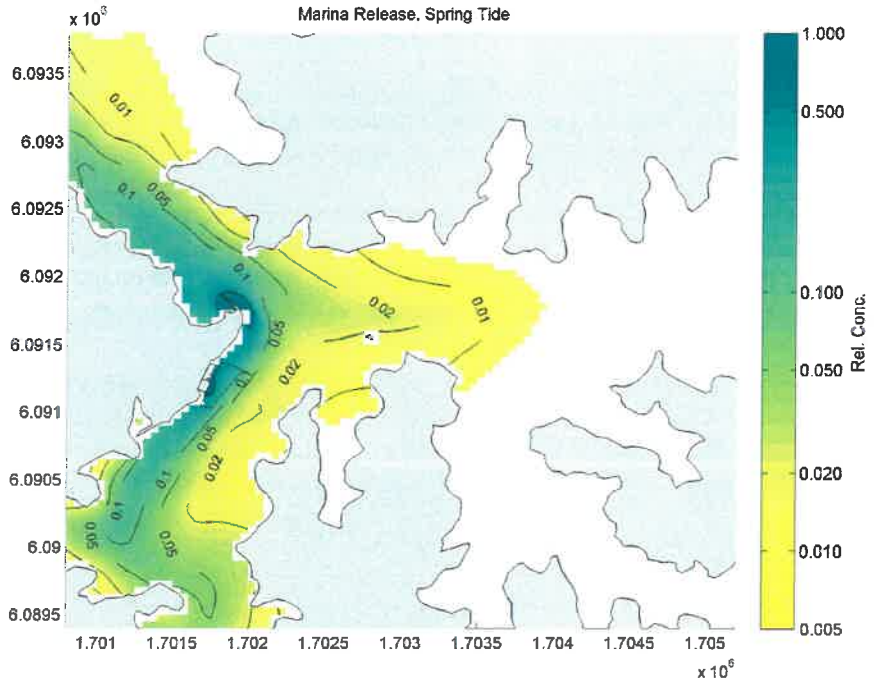

Figure 6.31 Predicted envelop of mean relative concentration for a generalised contaminant plume emanating from the Stage 2 Marina under spring tides.

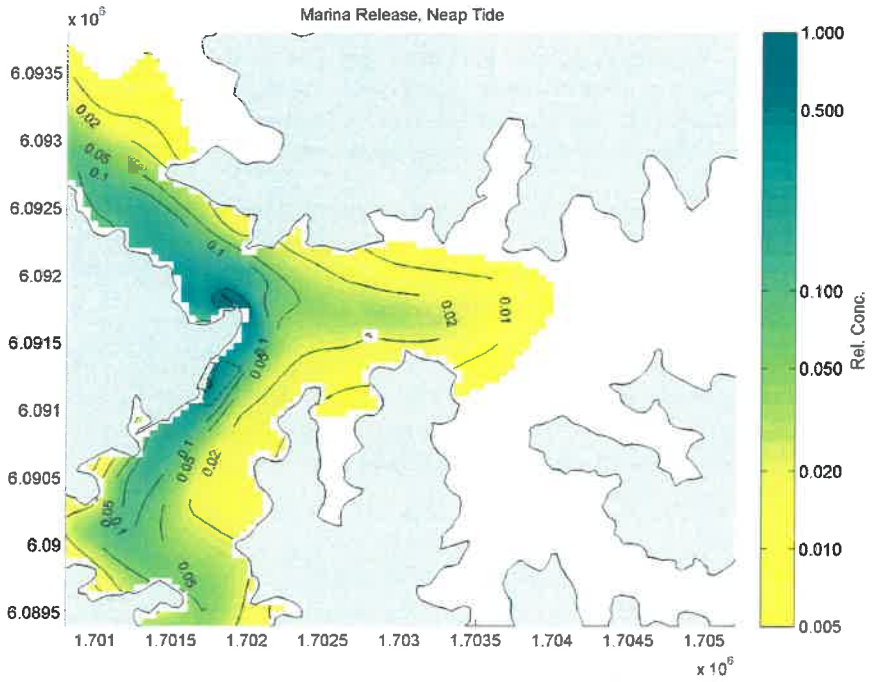

Figure 6.32 Predicted envelop of mean relative concentration for a generalised contaminant plume emanating from the Stage 2 Marina under neap tides.

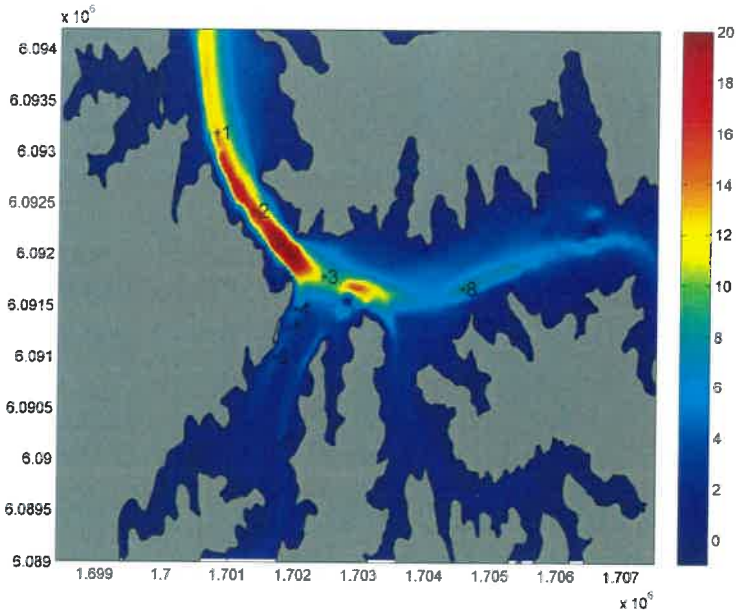

Figure 6.33 Sites used for Ptrack time-series plots for both the generic Marian contaminant release and the catchment sediment simulations.

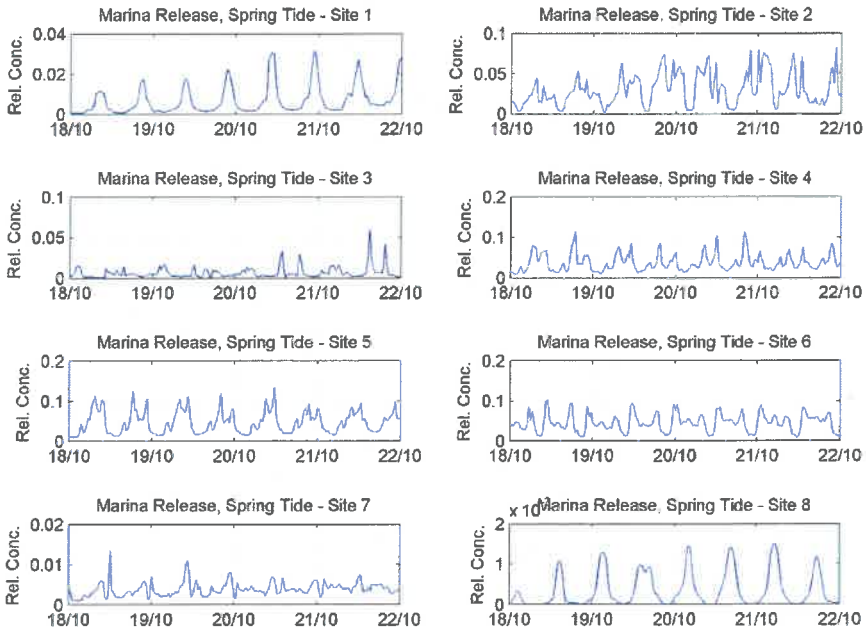

Figure 6.34 Predicted relative concentrations – marina release spring tide. Sites as shown in Figure 6.33.

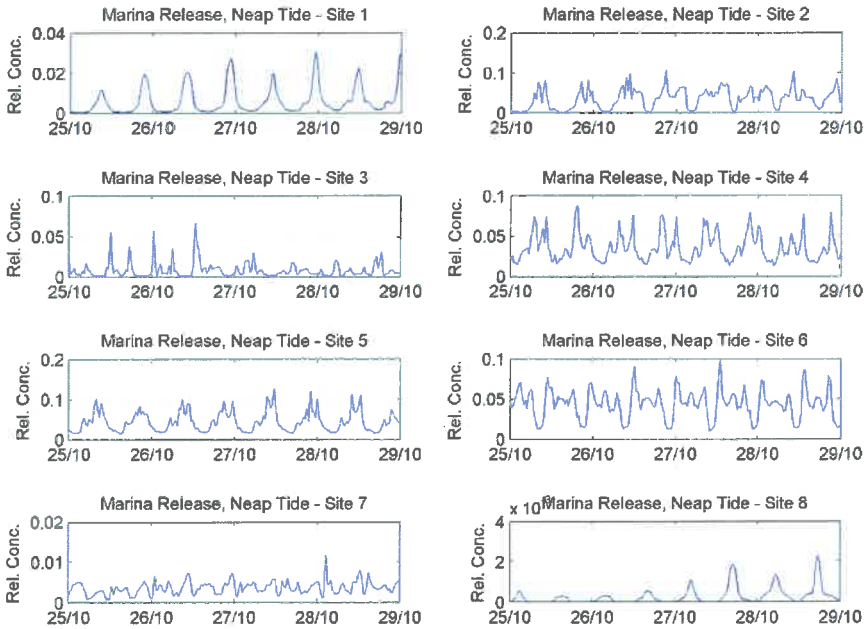

Figure 6.35 Predicted relative concentrations – marina release neap tide. Sites as shown in Figure 6.33.

6.5. Catchment sediment pathways

Ptrack simulations were carried out to quantify the effects of the Stage 2 development in terms of the potential pathway of catchment derived sediments. Release points were defined at the catchment sources for both the Kawakawa River and Waikare Inlet. Idealised source concentrations of 1.075 $kg.m^{-3}$ and 0.347 $kg.m^{-3}$ were assigned, based on the NIWA data (Section 2.3). Note that NIWA assumed an idealised Kawakawa River source concentration of 8.0 $kg.m^{-3}$ for a flood event – Ptrack results for the catchment source simulations under such flood conditions would thus be eight times those presented below.

Separate model runs were carried out for each catchment source and for each simulation a continuous release over a 7-day period was modelled beginning on a neap tide. Model results provide a probabilistic quantification of the physical mixing of catchment derived sediments within the Kawakawa River, Waikare Inlet and Veronica Channel. By comparing pre marina model results with results from the Stage 2 development the effects of the marina development on catchment derived sediment delivery can be assessed.

Using the variable kernel technique outlined in Section 3.2 the location of the particle cloud at each half-hour time-step during the seven-day simulation was used to define a mean concentration map for the complete simulation.

The resulting mean depth-averaged concentration maps for the Waikare and Kawakawa catchment sediment simulations are shown in Figure 6.36 and Figure 6.37 respectively. It can be seen that there is limited connection between Waikare Inlet catchment sediments and the Marina. This result is consistent with the Marina release results which showed very low plume concentrations within the Waikare Inlet for the Marina contaminant simulations.

Model results for the Kawakawa River simulations (Figure 6.37) show that the highest catchment derived sediment concentrations occur in the eastern channel of the Kawakawa River. Also note the relatively high sediment concentrations with the Waikare Inlet given a good indication of the role that the Kawakawa River catchment derived sediments have on the overall sediment dynamics of the area. The extent of the Kawakawa River sediment plume for the pre Marina and Stage 2 development simulations indicate that overall the development of the Marina has little effect on the delivery of Kawakawa catchment sediments.

At the sites shown in Figure 6.33 the time-series plots of predicted concentrations for both the Kawakawa and Waikare simulations are shown in Figure 6.38 and Figure 6.39 respectively.

For the Kawakawa catchment simulation (Figure 6.38) maximum predicted concentrations at Site 7 (the closest to the source) occur during neap tides. As tide range increases stronger tidal flows and greater exchange of water during tidal cycles provides greater flushing of the Kawakawa River, leading to reduced sediment concentrations at this site.

At all other sites the clear ebb tide modulation of the predicted concentrations is evident.

Comparing the predictions for the pre marina configuration and the Stage 2 results it can be seen that there are small changes (both increases and decreases) at different states of tide and tidal range. Maximum concentration values (occurring at low tide) are subtlety changed but overall the dynamics of the sediment delivery to the Marina site is not significantly altered (Sites 4-6, Figure 6.38) with the Stage 2 development of the Marina.

For the Kawakawa catchment simulation (Figure 6.39) the distribution of the predicted sediment concentrations during low tide is slightly changed. At all other sites very low concentrations are predicted to occur showing the high degree of dilution that occurs for Waikare Inlet derived sediments.

Overall the proposed development of the Marina has very little effect on the nature of the sediment delivery for both the Waikare Inlet and Kawakawa River catchments. Sediment delivered to the Marina is via the Kawakawa River catchment and the total quantity of sediment being transported to the Marina site is not significantly altered with the Stage 2 development.

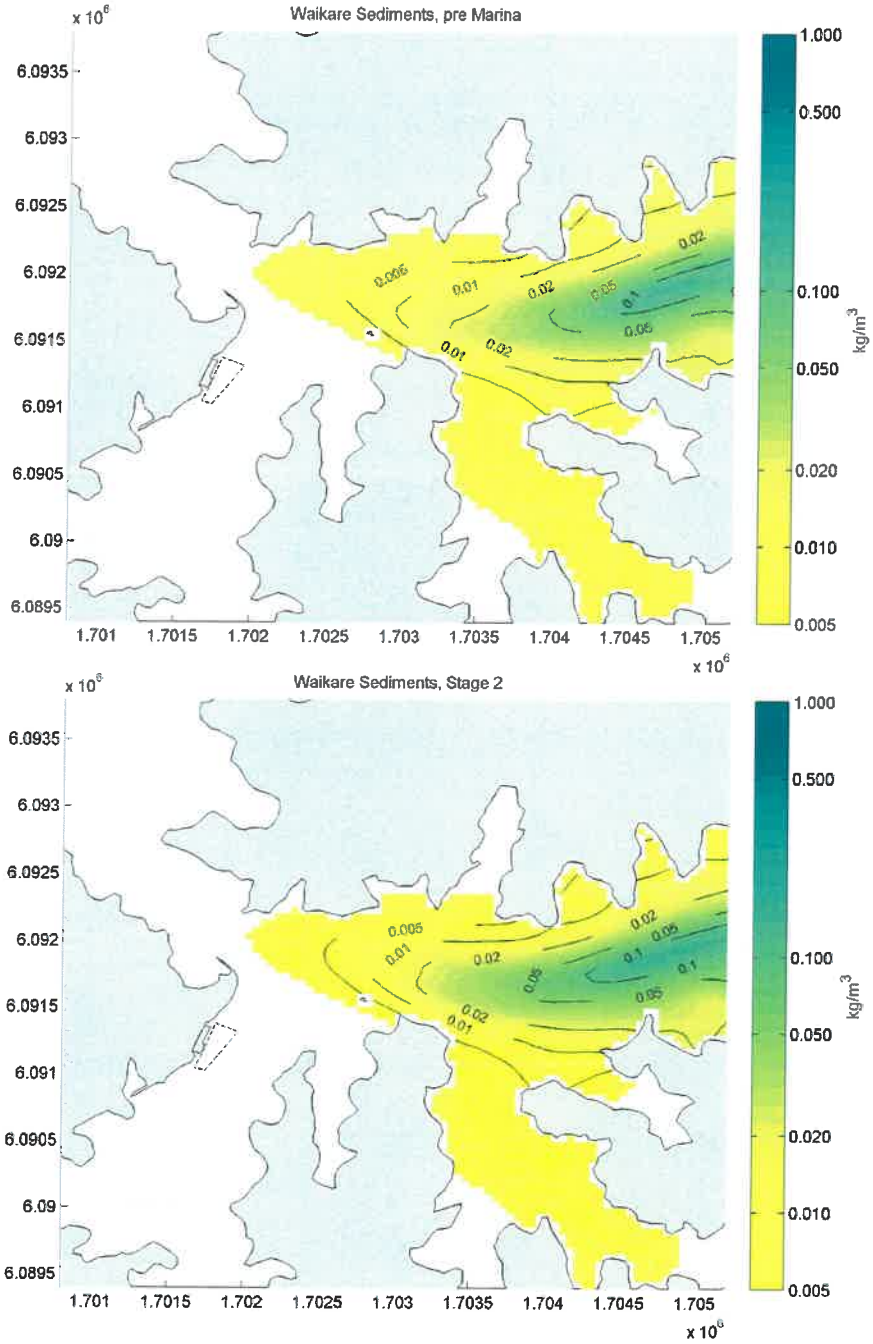

Figure 6.36 Predicted mean suspended sediment concentrations for Waikare Inlet catchment sediment simulation. Top panel shows predictions for the pre Marina conditions and bottom panel shows results with the Stage 2 development.

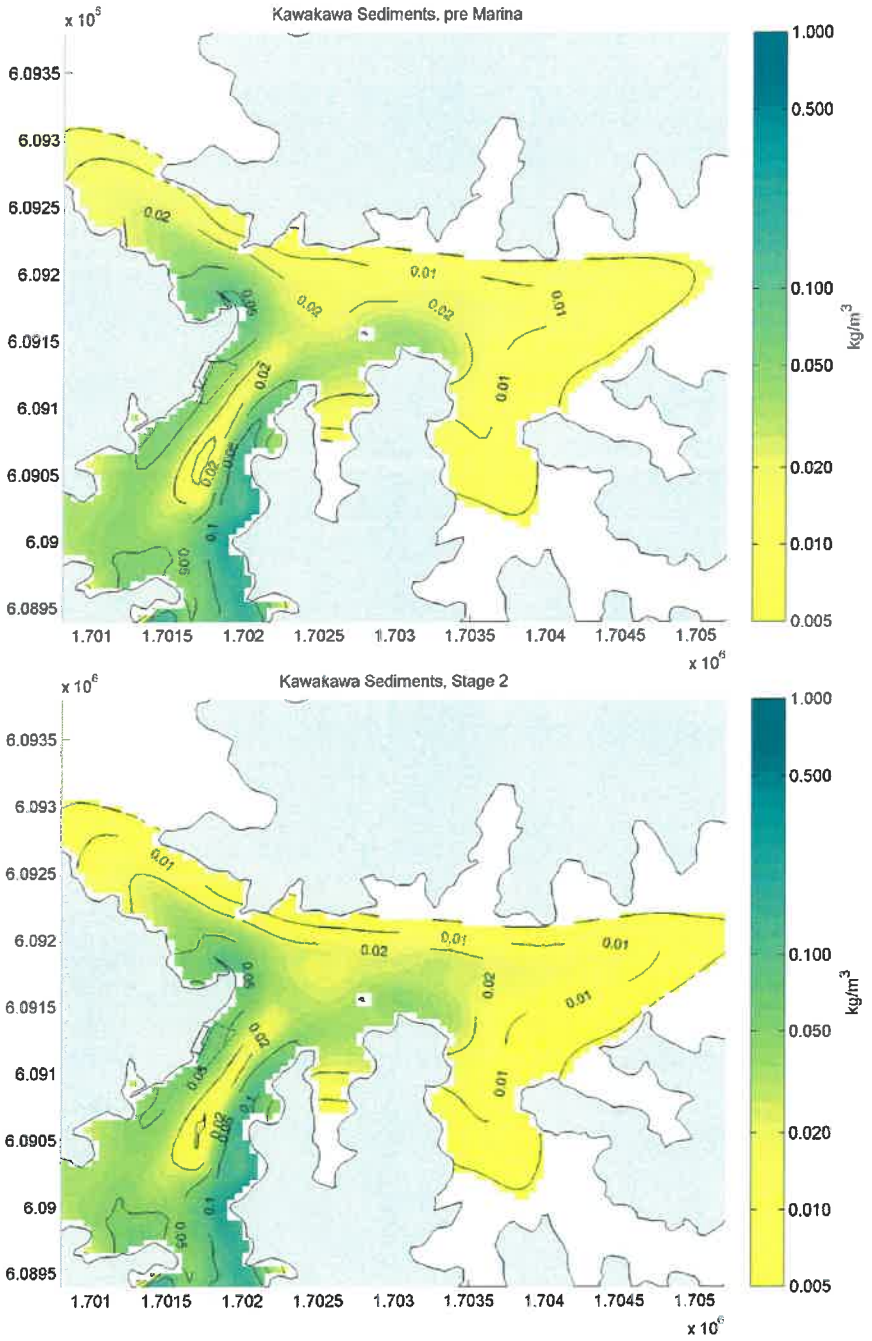

Figure 6.37 Predicted mean suspended sediment concentrations for Kawakawa River catchment sediment simulation. Top panel shows predictions for the pre Marina conditions and bottom panel shows results with the Stage 2 development.

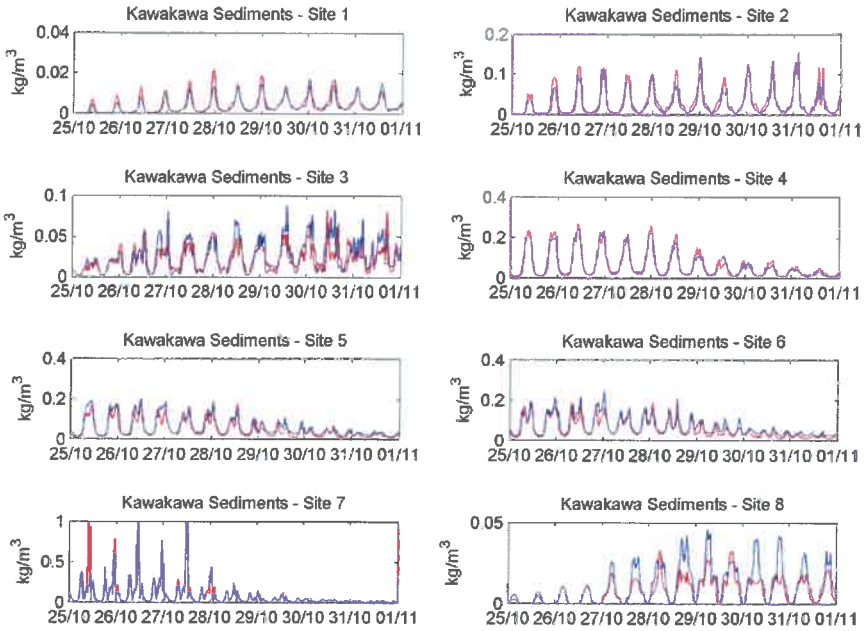

Figure 6.38 Predicted sediment concentrations for Kawakawa River catchment sediment release. Sites as shown in Figure 6.33. Blue line shows predictions prior to the Marina being built and the red line shows predictions with the Stage 2 development in place.

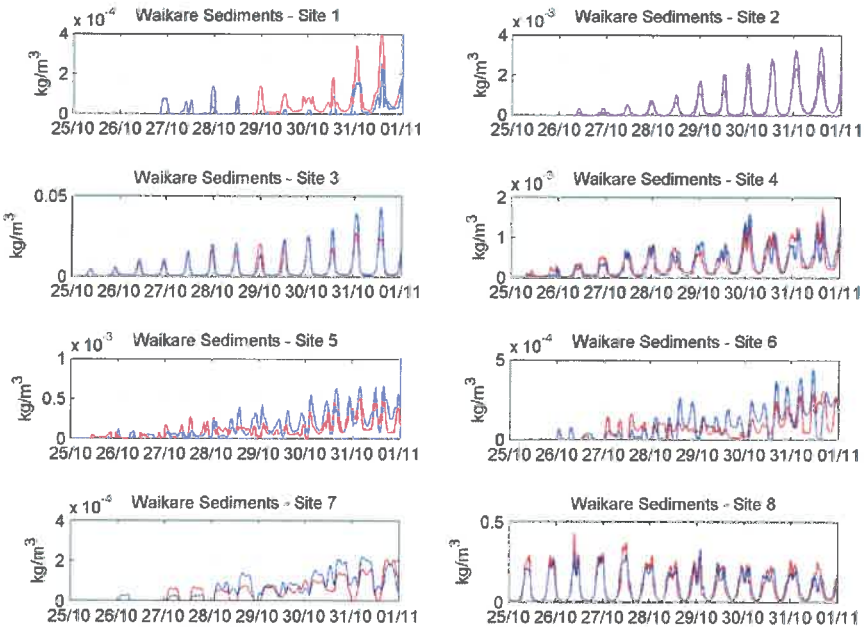

Figure 6.39 Predicted sediment concentrations Waikare Inlet catchment sediment release. Sites as shown in Figure 6.33. Blue line shows predictions prior to the Marina being built and the red line shows predictions with the Stage 2 development in place.

6.6. Marina sediment dynamics

In terms of the sediment dynamics within the Marina area there are five zones of interest;

1. An area of maximum observed deposition occurs near the wave screen to the north of the existing Marina (Figure 2.3). Model results indicate that sediment delivery to this area will be unchanged and the predicted sediment transport capacity remains unchanged (e.g. Figure 6.18). Deposition in this area is likely to continue at the observed rate of the order of +30 mm/yr.

2. Within the existing Marina maximum sediment transport capacity occurs within the south-west corner of the Marina (Figure 6.19). These higher transport rates imply that sediment is unlikely to deposit in these areas and in fact may be responsible for the observed erosion seen inshore of the southern end of the existing Marina. With the development of the Stage 2 Marina sediment transport rates in this area are reduced (e.g. Figure 6.29) but remain relatively high (Figure 6.30). The observed bed level changes of around -10 mm/yr are likely to be slightly reduced in this area.

3. Within the offshore zone of the Stage 2 Marina small changes in sediment transport capacity occur (e.g. Figure 6.29) so the observed deposition rates averaging around 5 mm/yr are likely to continue in this area.

4. Offshore of the proposed reclamation the pattern of predicted sediment transport capacity rates are altered with the Stage 2 development (Figure 6.19 and Figure 6.30). However the magnitude of the predicted sediment transport capacities is not significantly altered. The observed average bed level changes of around 5 mm/yr in this area (Figure 2.3) are likely to continue.

5. Between Ashbys Boat and the south-east corner of the reclamation model predictions indicate that the sediment transport capacity will increase (e.g. Figure 6.29). The observed deposition rates immediately north of Ashbys (10-20 mm/yr) are therefore likely decrease.

7. SUMMARY

Using a calibrated hydrodynamic model of the Bay of Islands with three different bathymetry configurations (pre marina, existing Marina and proposed Stage 2 Marina) the effects of the Marina development in terms of changes in tidal currents and the potential for sediment transport have been quantified.

Outputs from hydrodynamic simulations have been used to drive a particle tracking model to determine how conservative contaminants released from within the Stage 2 development may mix within the Kawakawa River, Waikare Inlet and Veronica Channel. Model results give an indication of the potential extent of any contaminant plume emanating from the Marina and quantify the degree of dilution achieved at key locations both in the vicinity of the Marina and remotely.

In addition the particle tracking model has been used to simulate the transport of catchment derived sediments through the Kawakawa River and Waikare Inlet. Model results quantify if the development of the Marina in any way affects the transport of sediments within the Bay of Islands system.

Tidal Currents

- Maximum changes in tidal flows of less than 0.05 $m.s^{-1}$ are predicted to occur due to the marina development. Changes in flow outside of the Marina area are restricted to the area immediately offshore of the marina within the Kawakawa River.

- Changes to residual tidal currents of less than 0.005 $m.s^{-1}$ are predicted to occur within both the Marina area itself and the western channel of the Kawakawa River.

Marina Contaminants

- Ten-fold dilution is achieved within 1500 m south of the Marina along the western channel of the Kawakawa River.

- Limited dilution of contaminants occurs between the Marina, the Opua Wharf and Ferry Ramp.

- Along the southern shoreline of the Veronica Channel (towards English Bay) ten-fold dilution is achieved within 1300 m of the Wharf.

- Within the Veronica Channel itself and across the Kawakawa River relatively rapid dilution occurs.

- Predicted relative concentrations within the entrance to Waikare Inlet are less than 0.05 with rapid dilution occurring within the Inlet itself.

Dredge Plume

- During construction of the marina sediment plumes from the dredging operation will be transported along the western shoreline of the Kawakawa River, towards the Opua Wharf and Ferry Ramp, and along the foreshore to English Bay.

- The estimated source concentration (0.14 $kg.m^{-3}$) is comparable with the lower levels of suspended sediment concentrations observed during drought conditions within the Veronica Channel and well below the observed suspended sediment concentrations within the Waikare Inlet.

- Predicted mean suspended sediment concentrations are well below observed background levels (0.1-0.4 $kg.m^{-3}$) and an order of magnitude less than the average catchment source sediment concentrations.

- During river flood events suspended sediment concentrations within both the Kawakawa River and Waikare Inlet are likely to increase by a factor of eight compared to the observed dry weather levels of suspended sediment concentrations.

Catchment Sediments

- Model results indicate that overall the proposed development of the Marina has very little effect on the nature of the catchment derived sediment delivery to the wider Bay of Islands environs.

- The total quantity of catchment derived sediments being transported to the Marina site is not significantly altered with the development of the Stage 2 Marina.

Marina Sediment Dynamics

- Sediment deposition near the wave screen to the north of the existing Marina is likely to continue at the observed rate (of the order of +30 mm/yr) with the development of the Stage 2 Marina.

- Observed bed level changes within the south-west corner of the existing Marina of around -10 mm/yr are likely to be reduced with the development of the Stage 2 Marina.

- Within the offshore area of the Stage 2 Marina, observed deposition rates averaging around 5 mm/yr are likely to continue.

- Directly offshore of the proposed reclamation the observed average bed level changes of around 5 mm/yr are likely to continue with the development of the Stage 2 Marina.

- Immediately north of Ashbys boatyard the observed deposition rate of 10-20 mm/yr is likely to be reduced with the introduction of the reclamation.

REFERENCES

Christoffersen, J.B. and I.G. Jonsson. (1985) Bed Friction and Dissipation in a Combined Current and Wave Motion. Ocean Engineering 12(5):387-423.

DML (2011) Opua Marina Surveys 2005/2011 - Data conversion and comparisons. Report prepared for Far North Holdings.

García-Martínez, R. and Flores-Tovar, H. (1999) Computer modelling of oil spill trajectories with a high accuracy method. Spill Science & Technology Bulletin 5 (5): 6323–330.

Gross, E. S., Koseff, J. R., and Monismith, S. G. (1999) Three dimensional salinity simulations of South San Francisco Bay. J. Hydraulic Eng. 125~11, 1199–1209.

Kantha, L.H., and Clayson, C.A. (1994) An improved mixed layer model for geophysical applications. Journal of Geophysical Research: Oceans 99, 25235–25266.

Knight, B.R., Zyngfogel, R., and Forrest, B. (2009) PartTracker - a fate analysis tool for marine particles. Proceedings of Australasian Coasts and Ports Conference.

Lonin, S. A. (1999) Lagrangian model for oil spill diffusion at sea. Spill Science & Technology 5 (5-6): 331–336.

NIWA (2010) Bay of Islands OS20/20 survey report. Chapter 6: TRANS – Sediment Transport. NIWA Client Report WLG2010-38.

Pawlowicz, R., Bob Beardsley, B., and Lentz, S. (2002) Classical tidal harmonic analysis including error estimates in MATLAB using TTIDE. Computers & Geosciences 28, 929–937

Press, W. H., Flannery, B. P., Teukolsky, S. A. and Vetterling, W. T. (1992) Adaptive Stepsize Control for Runge-Kutta. Chapter 16.2 In: Numerical Recipes in FORTRAN 77: The Art of Scientific Computing, Cambridge University Press, ISBN 0-521-43064-X.

Raudkivi, A. J. (2005) Report on the Hydraulic Aspects of the Opua Marina Extension.

Soulsby, R., 1997. Dynamics of marine sands, a manual for practical applications. Thomas Telford, London

Song, Y. and Haidvogel, D. B. (1994) A semi-implicit ocean circulation model using a generalized topography-following coordinate system. J. Comp. Phys., 115(1), 228-244.

Vitali, L., Monforti, F., Bellasio, R., Bianconi, R., Sachero, V., Mosca, S. and Zanini, G. (2006) Validation of a Lagrangian dispersion model implementing different kernel methods for density reconstruction. Atmospheric Environment 40: 8020-8033.

Zhang, Y.L., and Baptista, A.M. (2008). A semi-implicit Eulerian-Lagrangian finite element model for cross-scale ocean circulation. Ocean Modelling 21, 71–96.

Zhang, A., Hess K.W., and Aikman F. (2010). User-based skill assessment techniques for operational hydrodynamic forecast systems. Journal of Operational Oceanography. Volume 3. 11-24.

APPENDIX 1 – HYDRODYNMIC TIME SERIES PLOTS

Time series plots of predicted depth-averaged currents at ten selected time-series sites (Table 6.1).

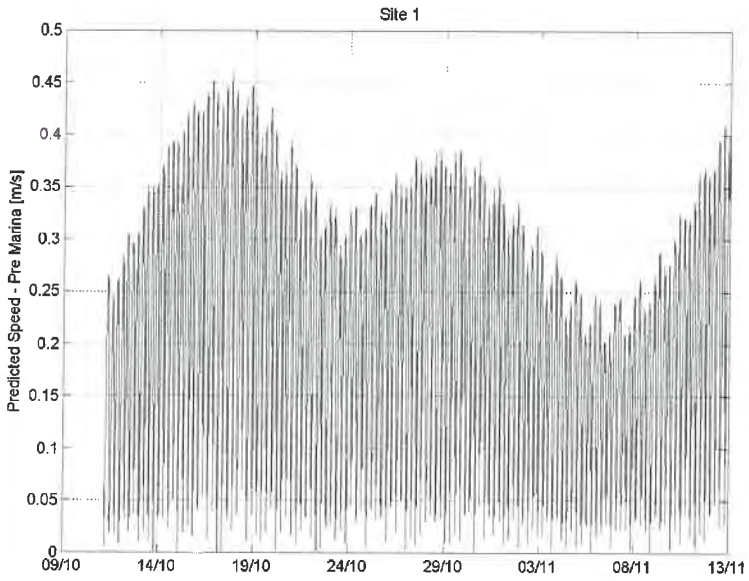

Figure A1 Predicted depth-averaged speed at Site 1 (Figure 6.8)

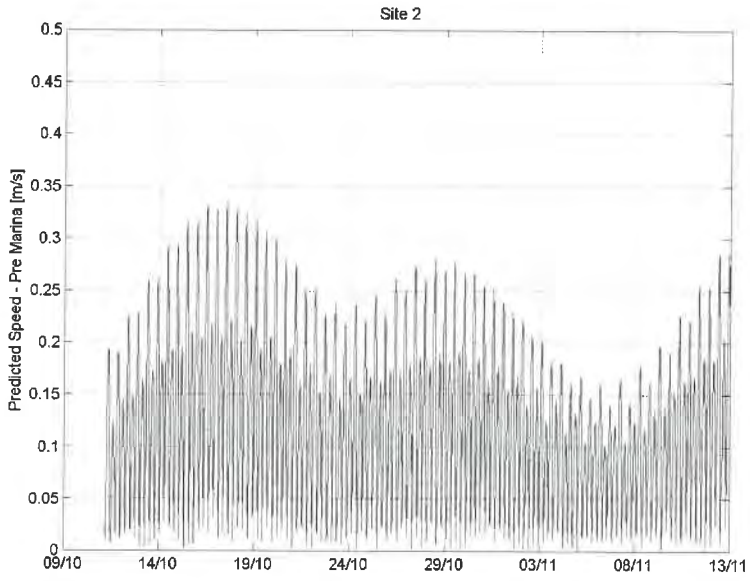

Figure A2 Predicted depth-averaged speed at Site 2 (Figure 6.8)

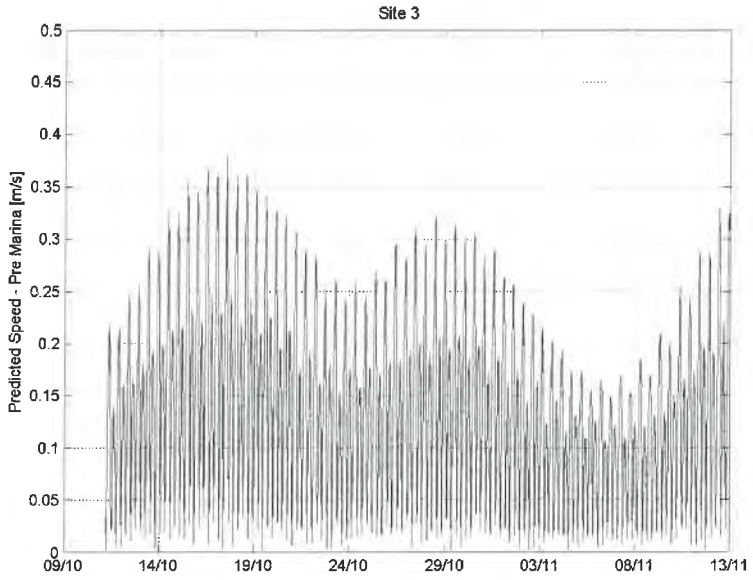

Figure A3 Predicted depth-averaged speed at Site 3 (Figure 6.8)

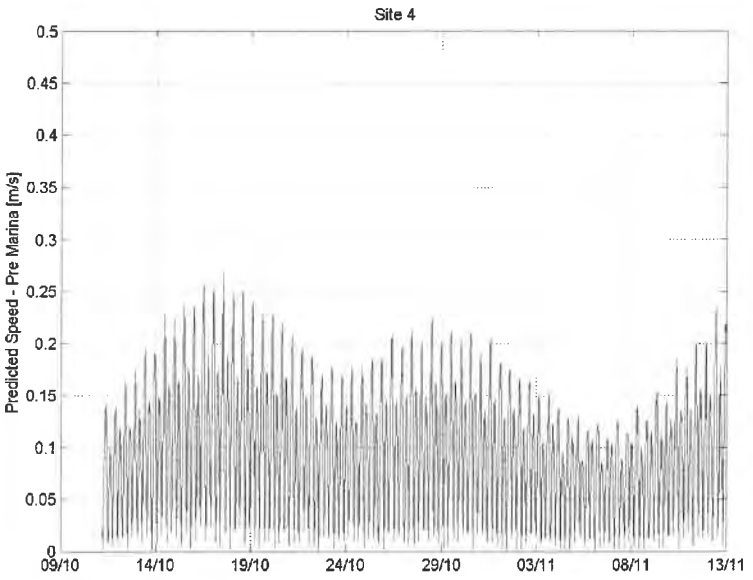

Figure A4 Predicted depth-averaged speed at Site 4 (Figure 6.8)

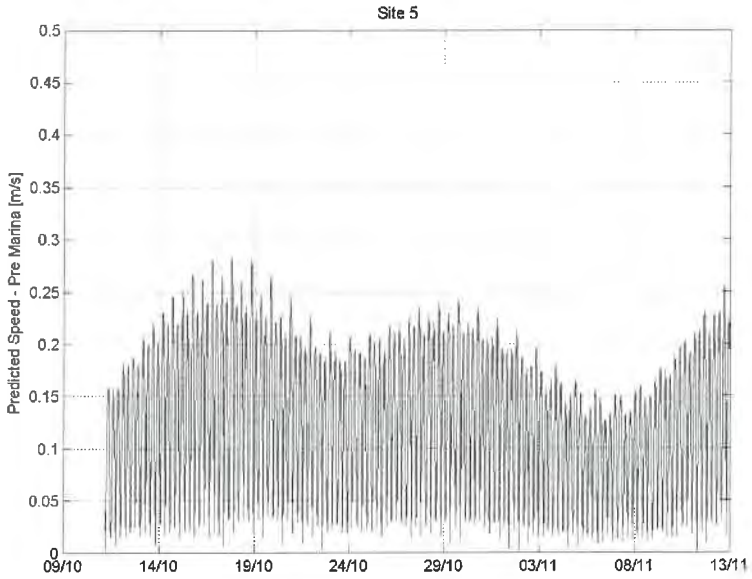

Figure A5 Predicted depth-averaged speed at Site 5 (Figure 6.8)

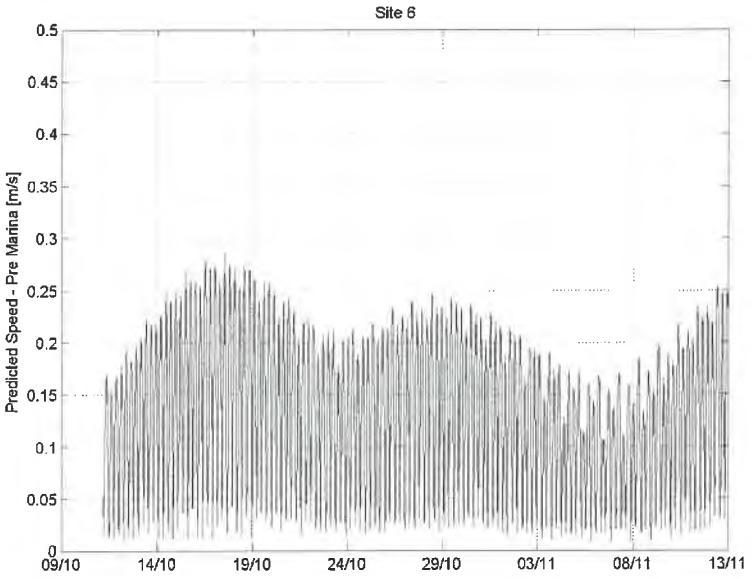

Figure A6 Predicted depth-averaged speed at Site 6 (Figure 6.8)

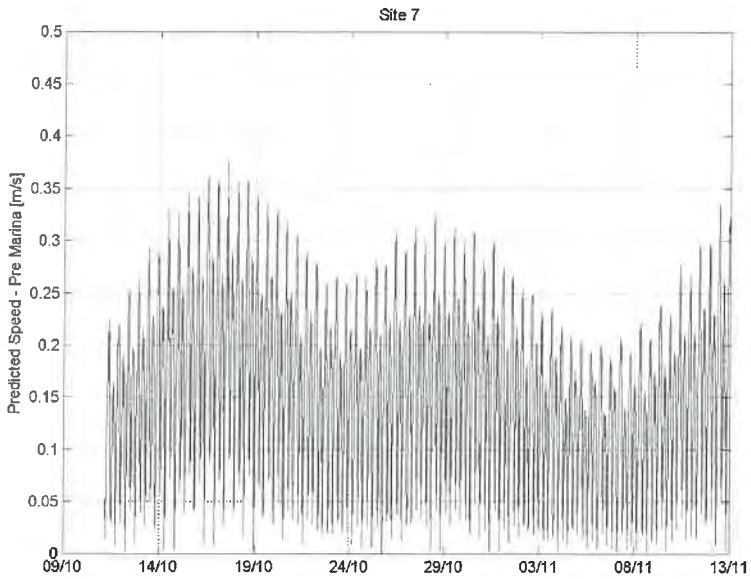

Figure A7 Predicted depth-averaged speed at Site 7 (Figure 6.8)

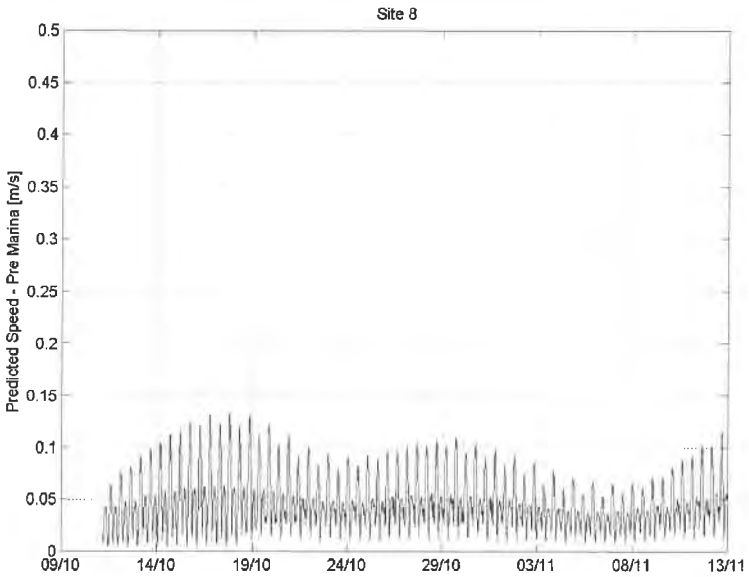

Figure A8 Predicted depth-averaged speed at Site 8 (Figure 6.8)

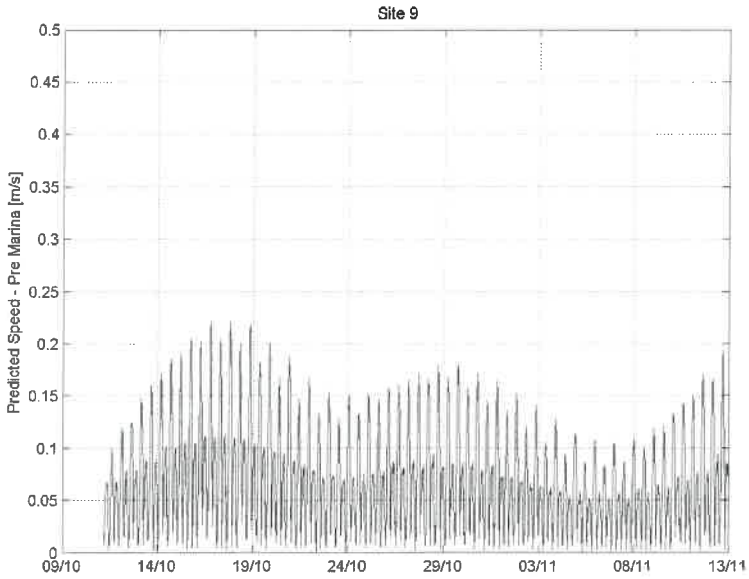

Figure A9 Predicted depth-averaged speed at Site 9 (Figure 6.8)

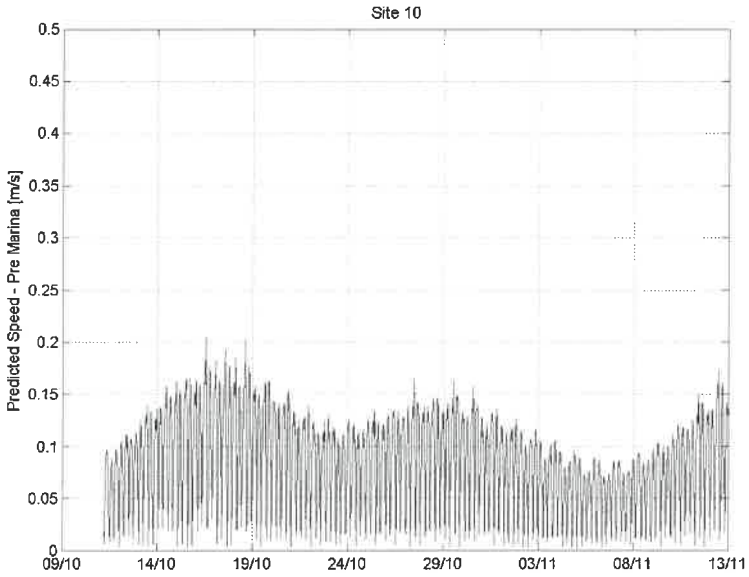

Figure A10 Predicted depth-averaged speed at Site 10 (Figure 6.8)